

Two-Year Longitudinal Monitoring of Amnesic Mild Cognitive Impairment Patients with Prodromal Alzheimer's Disease Using Topographical Biomarkers Derived from Functional Magnetic Resonance Imaging and Electroencephalographic Activity

Jorge Jovicich^{a,1,*}, Claudio Babiloni^{b,c,1,*}, Clarissa Ferrari^d, Moira Marizzoni^e, Davide V. Moretti^f,
Claudio Del Percio^g, Roberta Lizio^b, Susanna Lopez^b, Samantha Galluzzi^c, Diego Albani^h,
Libera Cavaliere^c, Ludovico Minati^a, Mira Didic^{i,j}, Ute Fiedler^k, Gianluigi Forloni^h,
Tilman Henschl^l, José Luis Molinuevo^m, David Bartrés Faz^{n,o}, Flavio Nobili^{p,q}, Daniele Orlandi^e,
Lucilla Parnetti^r, Lucia Farotti^r, Cinzia Costa^r, Pierre Payoux^s, Paolo Maria Rossini^t,
Camillo Marra^l, Peter Schönknecht^l, Andrea Soricelli^g, Giuseppe Noce^g, Marco Salvatore^g,
Magda Tsolaki^u, Pieter Jelle Visser^v, Jill C. Richardson^w, Jens Wiltfang^{k,x,y}, Régis Bordet^z,
Olivier Blin^{aa} and Giovanni B. Frisoni^{e,ab} and the PharmaCog Consortium

^aCenter for Mind/Brain Sciences, University of Trento, Italy

^bDepartment of Physiology and Pharmacology "V. Erspamer", Sapienza University of Rome, Rome, Italy

^cDepartment of Neuroscience, IRCCS-Hospital San Raffaele Pisana of Rome and Cassino, Rome and Cassino, Italy

^dUnit of Statistics, IRCCS Istituto Centro San Giovanni di Dio Fatebenefratelli, Brescia, Italy

^eLab Alzheimer's Neuroimaging & Epidemiology, IRCCS Istituto Centro San Giovanni di Dio Fatebenefratelli, Brescia, Italy

^fAlzheimer's Epidemiology and Rehabilitation in Alzheimer's disease Operative Unit, IRCCS Istituto Centro San Giovanni di Dio Fatebenefratelli, Brescia, Italy

^gIRCCS SDN, Napoli, Italy

^hDepartment of Neuroscience, IRCCS - Istituto di Ricerche Farmacologiche Mario Negri, Milano, Italy

ⁱAix-Marseille Université, INSERM, INS UMR_S 1106, Marseille, France; Service de Neurologie et Neuropsychologie, APHM Hôpital Timone Adultes, Marseille, France

¹These authors contributed equally to this work.

*Correspondence to: Dr. Jorge Jovicich, Center for Mind/Brain Sciences, University of Trento, Trento, Italy. Tel.: +39 0461 28 3064; Fax: +39 0461 28 3066; E-mail: jorge.jovicich@unitn.it

and Dr. Claudio Babiloni, Department of Physiology and Pharmacology "Erspamer", University of Rome "La Sapienza", Rome, Italy. Tel.: +39 0649910989; Fax: +39 0649910917; E-mail: claudio.babiloni@uniroma1.it

- ^jAPHM, Timone, Service de Neurologie et Neuropsychologie, APHM Hôpital Timone Adultes, Marseille, France
- ^kDepartment of Psychiatry and Psychotherapy, LVR-Hospital Essen, Faculty of Medicine, University of Duisburg-Essen, Essen, Germany
- ^lDepartment of Psychiatry and Psychotherapy, University of Leipzig, Leipzig, Germany
- ^mAlzheimer's disease and other cognitive disorders unit, Neurology Service, ICN Hospital Clinic i Universitari and Pasqual Maragall Foundation Barcelona, Spain
- ⁿDepartment of Medicine, Medical Psychology Unit, Faculty of Medicine and Health Sciences, University of Barcelona, Barcelona, Spain
- ^oInstitut d'Investigacions Biomèdiques August Pi i Sunyer (IDIBAPS), Barcelona, Spain
- ^pDepartment of Neuroscience (DINOEMI), Neurology Clinic, University of Genoa, Italy
- ^qU.O. Clinica Neurologica, IRCCS Ospedale Policlinico San Martino, Genova, Italy
- ^rClinica Neurologica, Università di Perugia, Ospedale Santa Maria della Misericordia, Perugia, Italy
- ^sToNIC, Toulouse NeuroImaging Center, Université de Toulouse, Inserm, UPS, France
- ^tDepartment of Gerontology, Neurosciences & Orthopedics, Catholic University, Policlinic A. Gemelli Foundation-IRCCS, Rome, Italy
- ^u1st University Department of Neurology, AHEPA Hospital, Medical School, Aristotle University of Thessaloniki, Thessaloniki, Makedonia, Greece
- ^vDepartment of Neurology, Alzheimer Centre, VU Medical Centre, Amsterdam, The Netherlands
- ^wNeurosciences Therapeutic Area, GlaxoSmithKline R&D, Gunnels Wood Road, Stevenage, UK
- ^xDepartment of Psychiatry and Psychotherapy, LVR-Hospital Essen, Faculty of Medicine, University of Duisburg-Essen, Essen, Germany
- ^yDepartment of Psychiatry and Psychotherapy, University Medical Center (UMG), Georg-August-University, Goettingen, Germany
- ^zUniversity of Lille, Inserm, CHU Lille, U1171 - Degenerative and vascular cognitive disorders, Lille, France
- ^{aa}Aix Marseille University, UMR-CNRS 7289, Service de Pharmacologie Clinique, AP-HM, Marseille, France
- ^{ab}Memory Clinic and LANVIE - Laboratory of Neuroimaging of Aging, University Hospitals and University of Geneva, Geneva, Switzerland

Accepted 17 July 2018

Abstract. Auditory “oddball” event-related potentials (aoERPs), resting state functional magnetic resonance imaging (rsfMRI) connectivity, and electroencephalographic (rsEEG) rhythms were tested as longitudinal functional biomarkers of prodromal Alzheimer’s disease (AD). Data were collected at baseline and four follow-ups at 6, 12, 18, and 24 months in amnesic mild cognitive impairment (aMCI) patients classified in two groups: “positive” (i.e., “prodromal AD”; $n = 81$) or “negative” ($n = 63$) based on a diagnostic marker of AD derived from cerebrospinal samples ($A\beta_{42}/P$ -tau ratio). A linear mixed model design was used to test functional biomarkers for Group, Time, and Group \times Time effects adjusted by nuisance covariates (only data until conversion to dementia was used). Functional biomarkers that showed significant Group effects (“positive” versus “negative”, $p < 0.05$) regardless of Time were 1) reduced rsfMRI connectivity in both the default mode network (DMN) and the posterior cingulate cortex (PCC), both also giving significant Time effects (connectivity decay regardless of Group); 2) increased rsEEG source activity at delta (<4 Hz) and theta (4–8 Hz) rhythms and decreased source activity at low-frequency alpha (8–10.5 Hz) rhythms; and 3) reduced parietal and posterior cingulate source activities of aoERPs. Time \times Group effects showed differential functional biomarker progression between groups: 1) increased rsfMRI connectivity in the left parietal cortex of the DMN nodes, consistent with compensatory effects and 2) increased limbic source activity at theta rhythms. These findings represent the first longitudinal characterization of functional biomarkers of prodromal AD relative to “negative” aMCI patients based on 5 serial recording sessions over 2 years.

Keywords: Alpha rhythms, amnesic mild cognitive impairment, biomarkers, clinical trial, electroencephalography, functional magnetic resonance imaging, oddball event-related potentials, PharmaCog project, prodromal Alzheimer’s disease, resting state

INTRODUCTION

The International Working Group has recently made a useful distinction between diagnostic and topographical biomarkers of Alzheimer's disease (AD) for research applications in patients with amnesic mild cognitive impairment (aMCI) due to the prodromal manifestation of the pathology [1]. Diagnostic biomarkers were defined as those measuring *in vivo* intrinsic pathophysiological variables characterizing neurobiologically AD, namely amyloid deposition and neurofibrillary tangles in the brain. They are expected to be present at all stages of the disease, are observable even in the preclinical asymptomatic state, are not necessarily correlated with disease severity, and are indicated for inclusion of AD patients in clinical trial protocols. Diagnostic biomarkers include low doses of $A\beta_{1-42}$ and high doses of total tau (T-tau) or phospho-tau (P-tau) in cerebrospinal fluid (CSF) or evidence of significant amyloid deposition and tau aggregation in the brain in maps of positron emission tomography (PET) [2].

In contrast, topographic or progression biomarkers may not be specific of AD neuropathology or absent in early disease stages, but they can be very useful to monitor the progression of the disease in the brain and may be related to the kind and severity of cognitive deficits [1]. Progression markers include hippocampal atrophy or cortical thickness, assessed by structural MRI, and cortical hypometabolism in posterior cingulate, parietal, temporal, and hippocampal regions, measured by FDG-PET [1]. Of note, these topographic biomarkers are limited in the sense that they do not directly measure brain amyloid deposition and neurofibrillary tangles in AD patients, so they cannot be used as primary neuropathological endpoints in the evaluation of AD-modifying agents.

Promising candidates as topographic markers of AD are those reflecting functional aspects of brain neurotransmission, neural synchronization, and connectivity, as human cognition is the result of collective and coordinated processes within brain networks such as segregation and integration of cellular signaling [3–5]. In this line, functional MRIs accompanying a resting state condition in quiet wakefulness (rsfMRI) can be used for the computation of temporal correlations of blood oxygenation level dependent (BOLD) signals between voxels belonging to brain regions as a biomarker of intrinsic (not related to events) functional connectivity between those regions [6, 7]. Among various cerebral neural networks emerging from such rsfMRI analysis, the

default mode network (DMN) is of interest for clinical applications to AD research, being non-invasive and repeatable over time even in patients with several cognitive deficits. Previous rsfMRI studies have shown that this network includes nodes in posterior and anterior cingulate areas, angular gyri, occipital, and parietotemporal regions [8]. In the resting state condition, the intrinsic DMN functional connectivity may be associated with specific self-related and internal processes that can be parcellated into several sub-classes including self-awareness or “mental self” [9, 10] (defined as the conscious ability of reflecting/monitoring about one's sense of self regarding one's abilities, traits, and attitudes that guides behaviors, choices, and social interactions), self-reflective thought [11, 12], stimulus-independent thoughts [13], mind-wandering [14], introspection [15], integration of cognitive processes [16], and considering the thoughts and perspectives of others [17–19].

Other candidate topographic biomarkers of AD derive from electroencephalographic (EEG) techniques, which are noninvasive, cost-effective, and can be repeated several times along disease progression without learning effects affecting paradigms using tasks. When compared to fMRI and FDG-PET, EEG techniques recording scalp potentials have a modest spatial resolution of some centimeters but a very high temporal resolution (milliseconds); that temporal resolution is ideal to investigate cortical EEG rhythms at different frequency bands within about 1–40 Hz during a resting state condition (i.e., resting state EEG, rsEEG) and quick brain dynamics reflected by positive and negative voltage peaks within tens to hundreds of milliseconds in response to cognitive-motor events challenging attention, short episodic memory, and sensorimotor integration (i.e., event-related potentials, ERPs). A popular ERP paradigm used to investigate temporal dynamics of neural synchronization underpinning cognitive processes is the auditory oddball task [20]. In such a paradigm, subjects are administered a sequence of sensory stimuli of two classes, namely those with high (e.g., 80%) and low (e.g., 20%) probability to occur, with the instruction to pay attention and react (e.g., hand motor responses or mental stimulus) only to the rare ones considered as “targets” [21]. The extraction of variables of interest from rsEEG and ERPs requires different procedures of data analysis and source estimation, mainly based on frequency (rsEEG) and time (ERP) domains [22]. Derived rsEEG/ERP biomarkers may reflect synchronization and connectivity between large populations of cortical

pyramidal neurons during resting state or cognitive tasks [22].

Previous studies have shown that compared to control seniors, patients with aMCI and dementia due to AD were characterized by increased rsEEG power density at delta (<4 Hz) and theta (4–7 Hz) frequency bands in widespread cortical regions as well as decreased rsEEG power density at alpha (8–13 Hz) and beta (14–30 Hz) frequency bands in central and posterior cortical regions [22–32]. Concerning the oddball paradigm, these patients were characterized by ERP peak latency increase, amplitude decrease, and abnormal topography in a late ample positive component (i.e., P3b). Specifically, P3b peaks at about 300–400 ms from the onset of rare (20–30% of probability) auditory or visual stimuli [33–38]. As topographic biomarkers of progression, these rsEEG/ERP readouts pointed to increased abnormalities in delta/alpha rhythms and P3b peak in aMCI and AD patients with dementia at about 1-year follow up [27, 28, 34, 36]. These effects were typically discussed in relationship to death of cortical neurons, axonal pathology, and cholinergic neurotransmission deficits [29, 39–45].

Linear Mixed Models (R-package lme4) were used as statistical tests as they allow the use of individual longitudinal data sets even when some recording sessions are missing in the series (e.g., for technical failures or patients' problems). The mentioned findings motivate the evaluation of rsfMRI and rsEEG/P3b as topographic biomarkers sensitive to prodromal (MCI) and dementia stages of AD. This process needs to overcome the following methodological limitations of typical multi-centric longitudinal studies: 1) retrospective nature, 2) the use of few recording sessions over time (mostly a baseline and a 1-year follow up) subjected to the confounding effect of disease onset and trajectories in aMCI patients, 3) the lack of a careful characterization of aMCI due to AD as cognitive profile (only one test of episodic memory) and positivity to standard diagnostic biomarkers of AD, and 4) the absence of a control group of aMCI patients not due to AD with expected different disease evolution over time. The European, prospective, multi-centric study entitled "PharmaCog - E-ADNI" (<http://www.pharmacog.org>) addressed such limitations. In the PharmaCog study, 147 aMCI patients were screened as APOE genotyping and AD diagnostic markers of CSF and followed longitudinally with clinical, neuropsychological, MRI, rsEEG/ERP, and blood markers for 24 months. The aMCI patients were

separated into two sub-groups, namely those "positive" (i.e., prodromal AD) and "negative" to CSF diagnostic markers of AD (i.e., statistical thresholds for A β ₄₂/P-tau ratio based on APOE ϵ 4 carrier status [49]). Preparatory PharmaCog studies described the successful multisite MRI harmonization efforts [46–51] and the characterization of the "positive" and "negative" aMCI subjects as neuropsychological, MRI (i.e., hippocampal atrophy, morphometry, and diffusion), and rsEEG/ERP at the baseline stage [23, 52, 53].

This article is part of a Mini Forum on PharmaCog matrix of biomarkers of prodromal AD in patients with aMCI, which is based on four papers published in the *Journal of Alzheimer's Disease*. The specific aim of this article is to evaluate longitudinal functional topographical biomarkers derived from rsfMRI and rsEEG/ERP data in a population of aMCI enrolled in the PharmaCog project and test if these markers can differentiate the group of the "positive" aMCI patients with prodromal AD from the "negative" aMCI subgroup during a time window of 24 months with 5 serial recordings 6 months apart. A linear mixed model adjusted by nuisance covariates was used to investigate those functional biomarkers in terms of Group ("positive" versus "negative" differences regardless of time), Time (temporal effects regardless of Group effects), and Time \times Group fixed effects (differential progression between the two sub-groups). In the experimental design, the observation time (i.e., 24 months) was expected to account for possible different disease stages in the "positive" and "negative" aMCI patients, while the "negative" aMCI patients were used as a control subgroup. This allowed dissociating, at least in part, cognitive impairment and functional biomarker differences between prodromal and non-prodromal AD in the aMCI subgroups. For sample homogeneity, the statistical design included aMCI data only until conversion to dementia.

MATERIALS AND METHODS

Participants, clinical exams, and neuropsychological tests

Participants' demographics, clinical, and neuropsychological data have been described in recent PharmaCog studies [23, 52, 53]. Briefly, 147 aMCI patients were enrolled in 13 European memory clinics of the Innovative Medicine Initiative (IMI) PharmaCog project (<http://www.pharmacog.org>). Follow-up

233 examinations were performed every 6 months for at
234 least 2 years or until patient progressed to clinical
235 dementia. The main inclusion/exclusion criteria were
236 1) age between 55 and 90 years; 2) complaints of
237 memory loss by the patient, confirmed by a family
238 relative; 3) Mini-Mental State Examination (MMSE)
239 score of 24 and higher; 4) overall Clinical Dementia
240 Rating score of 0.5; 5) score on the logical memory
241 test lower than 1 standard deviation from the age-
242 adjusted mean; 6) 15-item Geriatric Depression Scale
243 score of 5 or lower; and 7) absence of significant other
244 neurologic, systemic or psychiatric illness.

245 *Functional MRI data*

246 The multi-site 3T rsfMRI acquisition and analysis
247 protocols have been described in recent studies from
248 the PharmaCog project, also demonstrating high test-
249 retest reproducibility across the Consortium with the
250 use of harmonized MRI acquisition protocols [48,
251 49]. Briefly, 13 European clinical sites equipped with
252 3.0T scanners used a harmonized MRI acquisition
253 protocol that included structural 3D T1 images [48]
254 and resting state echo-planar imaging (EPI) sessions
255 using manufacturer-provided sequences [49]. This
256 resulted in a sample of 882 rsfMRI datasets (147
257 subjects, 6 sessions per subject).

258 Standard brain data preprocessing was performed
259 using SPM8 (<http://www.fil.ion.ucl.ac.uk/spm>) run-
260 ning under Matlab R2012a (The MathWorks, Inc.,
261 Natick MA, USA) and code developed in-house [49].
262 The main focus of the analysis of rsfMRI data was
263 the functional connectivity within the nodes of DMN,
264 which is expected to be reduced in the early stages
265 of AD [23, 54–57]. In this line, DMN nodes of
266 interest for this study were the following: medial
267 prefrontal cortex (MFC), bilateral precuneus and pos-
268 terior cingulate cortex (PCC), and inferior left and
269 right parietal cortex (LPC and RPC, respectively). We
270 also included the left attention frontal-parietal (LFP)
271 network given its potential role in memory cogni-
272 tive reserve [23, 58]. The anatomical characteristics
273 of the DMN and LFP regions and the data analysis
274 procedure are reported in previous methodological
275 study of the Consortium [49]. In brief, Group Inde-
276 pendent component analysis (ICA) was performed
277 using 10 spatial components on the concatenated data
278 from each MRI site followed by back-reconstruction
279 [59] to derive the single session DMN and atten-
280 tion LFP network from each subject [49]. DMN
281 regions-of-interest (ROIs) for functional connectiv-
282 ity measurements were obtained by thresholding at

283 $z > 4$ the aggregate DMN site component [49]. For
284 each participant and session, this analysis yielded the
285 average connectivity z-score within the whole DMN,
286 LFP, and also considering separately each one of the
287 separate nodes within the DMN (PCC, LPC, RPC,
288 and MFC) [49]. These z-scores were used as func-
289 tional connectivity measures and were the rsfMRI
290 dependent variables in the statistical analyses.

291 The statistical analyses considered also two MRI-
292 related nuisance regressors for each session, the
293 white matter temporal signal-to-noise ratio (tSNR),
294 given its high variability across sites mostly driven
295 by hardware differences [49], and the median head
296 movement.

297 *EEG data*

298 Recordings of rsEEG (eyes-closed and -open;
299 $n = 126$) and auditory “oddball” ERPs ($n = 125$) were
300 performed by commercial digital EEG systems in
301 the Clinical Units of the PharmaCog Consortium
302 (see more details in [52]). A minimum of 19 scalp
303 electrodes was positioned according to the inter-
304 national 10–20 montage system and referenced to
305 linked earlobes or cephalic reference according to
306 the constraints of the local EEG systems. Ground
307 electrode was placed over the scalp, according to
308 the local standard of the Clinical Units. To moni-
309 tor eye movements and blinking, bipolar vertical
310 and horizontal electrooculograms (EOGs; 0.3–70 Hz
311 bandpass) were simultaneously recorded. Further-
312 more, a standard electrocardiographic (EKG) channel
313 was also recorded by a monopolar V6 derivation to
314 remove possible EKG artifacts from EEG data. All
315 electrophysiological data were digitized in contin-
316 uous recording mode (from 128 to 1000 Hz sampling
317 rate according to the constraints of the local EEG
318 systems). To minimize drowsiness and sleep onset,
319 the duration of the rsEEG recordings was established
320 subject-by-subject from at least 3 minutes to a maxi-
321 mum 5 minutes for each condition (i.e., eyes closed,
322 eyes open).

323 The rsEEG and ERP data were segmented and
324 analyzed offline in consecutive 2-s and 3-s epochs,
325 respectively. Artifactual epochs were identified using
326 a computerized home-made automatic software pro-
327 cedure [60], confirmed by two EEG experts (CDP,
328 RL), and then eliminated. Artefact-free rsEEG
329 epochs recorded during eyes open condition were
330 used to control the expected reactivity of alpha
331 rhythms as a sign of good quality of rsEEG record-
332 ings. Artefact-free rsEEG epochs recorded during

333 eyes open condition were used as an input for the
 334 analysis of EEG power density spectrum and cortical
 335 source estimation. Concerning ERPs, artifact-free
 336 ERP epochs related to frequent and rare stimuli were
 337 averaged separately to form individual ERPs for
 338 those two classes of auditory stimuli. The latency
 339 of the posterior P3b peak following rare stimuli was
 340 measured at the Pz electrode and used as a latency
 341 reference for further analysis. Based on that latency
 342 peak, voltage amplitude was measured at all scalp
 343 electrodes in both ERPs related to rare stimuli and
 344 those related to frequent stimuli. For ERP source
 345 estimation, individual P3b peak potential distribution
 346 was computed according to a standard procedure as
 347 the subtraction of P3b peak voltage for the rare stim-
 348 uli minus the potential distribution for the frequent
 349 stimuli at the same latency.

350 Official exact low-resolution brain electromag-
 351 netic tomography (eLORETA) freeware [61] was
 352 used for the estimation of cortical sources of the
 353 rsEEG and P3b peak data in a standard brain atlas
 354 [61]. This option made the present results replicable
 355 by anyone. However, more realistic brain mod-
 356 els may ensure more accurate source localizations
 357 (e.g., see [62–64]). eLORETA estimated the follow-
 358 ing rsEEG/P3b peak markers: 1) activity of global and
 359 regional (i.e., frontal, central, parietal, occipital, tem-
 360 poral, and limbic lobes as defined in the eLORETA
 361 brain atlas [61]) normalized cortical (eLORETA)
 362 sources of rsEEG rhythms for delta (2–4 Hz), theta
 363 (4–7 Hz), alpha 1 (8–10.5 Hz), delta/alpha 1, and
 364 theta/alpha 1 bands, as indexes of cortical neural syn-
 365 chronization; and (2) activity of cortical sources of
 366 posterior parietal (i.e., Brodmann areas 5, 7, 39, and
 367 40) and posterior cingulate (Brodmann areas 31 and
 368 23) regions generating P3b peak voltage, as an index
 369 of cortical neural synchronization related to attention
 370 and short-term auditory episodic memory.

371 *Patients' classification in prodromal AD and* 372 *control aMCI patients*

373 As mentioned in the Introduction section, the aMCI
 374 patients were classified into two subgroups named
 375 “positive” (i.e., prodromal AD) and “negative” aMCI
 376 based on the results of a Mixture Linear Model with
 377 the p sets at <0.05 [65]. This Model determined the
 378 existence of one or more Gaussian populations of
 379 aMCI subjects based on the frequency distributions
 380 of CSF $A\beta_{42}/P$ -tau levels in the baseline recordings.
 381 According to this Model, the aMCI patients were
 382 denoted as “positive” aMCI (i.e., prodromal AD) with

383 CSF $A\beta_{42}/P$ -tau levels lower than 15.2 for APOE
 384 $\epsilon 4$ carriers and 8.9 for APOE $\epsilon 4$ non-carriers. The
 385 remaining aMCI patients were denoted as “negative”
 386 aMCI.

387 *Statistical analysis*

388 Statistical analyses were performed using SPSS
 389 software for descriptive statistics and R software
 390 (A language and environment for statistical comput-
 391 ing, version 3.4.1) for the computation of Mixture
 392 and Linear Mixed Models. Characteristics of the
 393 aMCI participants at the baseline recordings were
 394 assessed by parametric t -tests (or corresponding non-
 395 parametric Mann-Whitney) for continuous Gaussian
 396 (or non-Gaussian) distributed variables ($p < 0.05$) and
 397 by Chi-square tests for categorical data ($p < 0.05$).

398 Linear Mixed Models (R-package lme4) were used
 399 as statistical tests as they allow the use of individ-
 400 ual longitudinal data sets even when some recording
 401 sessions are missing in the series (e.g., for techni-
 402 cal failures or patients' problems). Specifically, these
 403 models evaluated whether rsfMRI and rsEEG/ERP
 404 functional topographic biomarkers can differentiate
 405 a “positive” aMCI (prodromal AD) subgroup rela-
 406 tive to a “negative” aMCI subgroup over 24 months.
 407 Furthermore, two different types of Linear Mixed
 408 Models were used with all available values of the
 409 rsfMRI, rsEEG/P3b peak, and clinical variables in the
 410 whole aMCI cohort. In the Models, the fixed effect
 411 Group included the two subgroups of “positive” and
 412 “negative” aMCI patients, while the fixed effect Time
 413 included the values of rsfMRI, rsEEG/P3b peak, and
 414 ADAScog13 for baseline recordings and follow-ups
 415 at 6, 12, 18, and 24 months. The aMCI patients even-
 416 tually progressing to dementia were no more called
 417 for subsequent follow ups in order to have a relatively
 418 homogeneous sample of data relative to aMCI condi-
 419 tion. Random intercept and random slope across the
 420 variables were used as random effects in the Models
 421 to account for individual differences in the biomark-
 422 ers and ADAScog13 values at baseline as well as for
 423 individual changes of those variables across all aMCI
 424 patients over follow-ups. All Models were adjusted
 425 for age, sex, and education. The output of the Linear
 426 Mixed Models was presented in terms of standard-
 427 ized β coefficient, corresponding p -value and, for the
 428 interaction factor only, effect size (pseudo h^2) calcu-
 429 lated as ratio of explained variability of interaction
 430 effect on total variability of each model.

431 The first Linear Mixed Models of rsfMRI and
 432 EEG biomarkers were conducted with Time, Group,

Table 1
Clinical and socio-demographic features of amnesic mild cognitive impairment (aMCI) patients receiving resting state functional magnetic resonance imaging recordings (rsfMRI) in the present study. Patients were stratified into cerebrospinal (CSF) A β ₄₂/P-tau “positive” and “negative” according to APOE4-specific cut-offs for carriers and non-carriers of APOE4 genotyping. See Methods section for more details

	“Negative” aMCI (n = 63)	“Positive” aMCI (n = 81)	<i>p</i> ^a
Age, mean (Standard Deviation, SD)	68.3 (8.4)	69.8 (6.3)	0.2
Sex, F/M, No.	36/27	46/35	1
Education, mean (SD)	10.0 (4.3)	11.1 (4.4)	0.1
APOE ϵ 4 carriers, No. (%)	3 (5)	63 (78)	<0.001
MMSE score, mean (SD)	27.1 (1.8)	26.2 (1.8)	0.006
ADAS-cog13, mean (SD) ^{b,c}	19.1 (5.9)	21.6 (8.1)	0.052
CSF biomarkers, mean (SD, pg/ml)			
A β ₄₂	949 (244)	495 (132)	<0.001
P-Tau	47 (15)	84 (38)	<0.001
T-tau	301 (149)	614 (394)	<0.001

^a Assessed by ANOVA (for continuous Gaussian distributed variables) or Kruskal-Wallis with Dunn correction (for continuous non-Gaussian distributed variables) and Chi-square tests (for categorical variables). ^b Range 0–85, with 0 as the best score. ^c Information was missing for 1 patient. MMSE, Mini-Mental State Evaluation; SD, standard deviation; ADAS-cog13, Alzheimer Disease Assessment Scale-Cognitive Subscale, version 13; A β ₄₂, amyloid- β ; APOE, apolipoprotein E; CSF, cerebrospinal fluid; P-tau, tau phosphorylated at threonine 181; T-tau, total tau; SD, standard deviation.

and Time \times Group interaction as fixed effects. The rsfMRI biomarkers were adjusted also for median head motion and white matter tSNR. The main interest was focused on functional biomarkers (i.e., rsfMRI, rsEEG/P3b peak) associated with the Group effects (regardless of Time), Time effects (regardless of Group), and the Time \times Group interaction (the differential progression of the positive aMCI subgroup relative to the negative aMCI subgroup). Specifically, the Group effect showed functional biomarkers distinguishing the two subgroups of aMCI patients regardless the Time effect, while the Group \times Time interaction unveiled those biomarkers characterizing the disease progression over-time in the “positive” aMCI subgroup (i.e., prodromal AD).

The second Linear Mixed Models of rsfMRI and EEG biomarkers tested if those functional biomarkers (independent variable) and Time effects predicted cognitive decline over time in the aMCI subgroups as revealed by ADAS-cog13 scores (dependent variable).

RESULTS

PharmaCog aMCI patients’ features

Diagnostic markers of CSF and APOE genotypes were available in 144 out of 147 aMCI patients of the PharmaCog/E-ADNI cohort, thus the final data

analyses were performed in 144 patients. The main demographic and clinical characteristics of these 144 aMCI patients are reported in Table 1. All of them underwent rsfMRI acquisitions, while a slightly smaller group underwent to rsEEG/ERP recordings ($n = 126$ patients). The main demographic and clinical characteristics of them are reported in Table 2. In both Tables, as mentioned above, the aMCI patients were aggregated in subgroups based on the baseline A β ₄₂, phospho-tau (P-tau), and total tau (T-tau) values in the CSF as a function of APOE genotype [65]. The two aMCI subgroups were defined according to a standard diagnostic marker of AD in CSF samples (A β ₄₂/P-tau ratio; [1]), based on the results of a Linear Mixture Model [49].

Table 3 reports the number of aMCI patients who converted to AD or other non-AD pathologies during the PharmaCog study. The “negative” aMCI patient group did not present conversions to dementia due to AD within 24 months, but presented 2–3% of conversions to dementia due to non-AD pathologies at 12-month follow up and 4–5% at 24-month follow up. In contrast, the “positive” aMCI patients (i.e., prodromal AD) showed 11% of conversion to dementia due to AD at 12-month follow up, 27–29% at 24-month-follow up, and no conversion to dementia due to non-AD pathologies within 24 months. These features are compatible with the use of 1 SD as a threshold of memory deficits in the present inclusion

Table 2

Clinical and socio-demographic features of aMCI patients undergone to resting state electroencephalographic (rsEEG) and event-related potential (ERP) recordings in the present study. These patients, a subgroup of those described in Table 1, were stratified into CSF A β ₄₂/P-tau “positive” and “negative” according to APOE4-specific cut-offs for carriers and non-carriers of APOE4 genotyping. See Methods section for more details

	“Negative” aMCI (n = 54)	“Positive” aMCI (n = 72)	p ^a
Age, mean (Standard Deviation, SD)	68.5 (8.5)	69.9 (6.0)	0.2
Sex, F/M, No.	30/24	42/30	0.8
Education, mean (SD)	9.9 (4.1)	11.0 (4.5)	0.2
APOE ϵ 4 carriers, No. (%)	3.7%	77.8%	<0.001
MMSE, mean (SD)	26.3 (2.2)	25.2 (2.2)	0.01
ADAS-cog13, mean (SD) ^b	20.2 (6.8)	23.1 (7.7)	0.04
CSF biomarkers, mean (SD, pg/ml)			
A β ₄₂	932 (253)	500 (132)	<0.001
P-tau	47 (15)	84 (36)	<0.001
T-tau	297 (151)	600 (316)	<0.001

^a Assessed by ANOVA (for continuous Gaussian distributed variables) or Kruskal-Wallis with Dunn correction (for continuous non-Gaussian distributed variables) and Chi-square tests (for categorical variables). ^b Range 0–85, with 0 as the best score. ADAS-cog13, Alzheimer Disease Assessment Scale-Cognitive Subscale, version 13; A β ₄₂, amyloid- β ; APOE, Apolipoprotein E; CSF, cerebrospinal fluid; P-tau, tau phosphorylated at threonine 181; T-tau, total tau; SD, standard deviation.

Table 3

Number of patients who converted from aMCI to dementia due to AD and other pathologies. These patients were stratified into CSF A β ₄₂/P-tau “positive” and “negative” according to APOE4-specific cut-offs for carriers and non-carriers of APOE4 genotyping. See Methods section for more details

aMCI patients with rsfMRI recordings	CSF A β ₄₂ /P-tau “negative” aMCI group	CSF A β ₄₂ /P-tau “positive” aMCI group
n	63	81
Converted in AD (12 months)	0.0% (n=0)	11.1% (n=9)
Converted in AD (24 months)	0.0% (n=0)	27.2% (n=22)
Converted in other dementias (12 months)	3.2% (n=2)	0.0% (n=0)
Converted in other dementias (24 months)	4.8% (n=3)	0.0% (n=0)
aMCI patients with rsEEG/ERP recordings	CSF A β ₄₂ /P-tau “negative” aMCI group	CSF A β ₄₂ /P-tau “positive” aMCI group
n	54	72
Converted in AD (12 months)	0.0% (n=0)	11.1% (n=8)
Converted in AD (24 months)	0.0% (n=0)	29.2% (n=21)
Converted in other dementias (12 months)	1.9% (n=1)	0.0% (n=0)
Converted in other dementias (24 months)	3.7% (n=2)	0.0% (n=0)

488 criteria [51]. As expected, a substantial percentage of
489 the “positive” aMCI patients (i.e., prodromal AD) of
490 the present study showed APOE ϵ 4 carriers (63%) in
491 line with previous large studies in AD patients [50].

492 *rsfMRI measures of functional cortical*
493 *connectivity in the PharmaCog aMCI patients*

494 Table 4 reports the results of a Linear Mixed
495 Model showing the variance explained in rsfMRI
496 measures of functional cortical connectivity by the

497 fixed effects of Group (“positive” versus “negative”
498 group differences regardless of time), Time (temporal
499 differences regardless of group), and Time \times Group
500 interaction (differential progression across groups)
501 in aMCI patients (PharmaCog population described
502 in Table 3) over the observation time (24 months, 5
503 recording session 6 months apart).

504 Concerning Group and Time, rsfMRI functional
505 connectivity in both the DMN and PCC showed sig-
506 nificant effects ($p < 0.05$). Specifically, Time effects
507 in DMN and PCC showed a global reduction of

Table 4

Resting state fMRI nodes showing significant functional connectivity effects explained by a Linear Mixed Model of longitudinal changes (baseline, 6, 12, 18, 24 months follow ups) in aMCI patients stratified into two groups (“positive” as prodromal AD and “negative” as a control group)

rsfMRI connectivity measure	Group		Time		Time × Group	
	Std β	p	Std β	p	Std β	p
PCC	-0,296	0,001	-0,089	0,040	-0,053	0,500
LPC	0,167	0,080	-0,063	0,130	0,186	0,013
DMN	-0,228	0,010	-0,101	0,015	0,012	0,877
LFP	-0,002	0,987	-0,131	0,011	0,030	0,747

The model included Group (A β ₄₂/P-tau ratio), Time, and Time × Group interaction as main predictors of interest adjusted by age, sex, baseline MMSE score, temporal signal-to-noise ratio, and mean fractional head displacement as nuisance variables. Significant ($p < 0.05$) fixed effects are emphasized in bold. DMN, default mode network (all nodes); PCC, posterior cingulate cortex; LPC, inferior left parietal cortex; LFP, left attention frontal-parietal network; Std β , standardized β coefficient of Linear Mixed Model.

functional cortical connectivity over time regardless of Group (DMN: $p = 0.01$, Std $\beta = -0.1$; PCC: $p = 0.05$, Std $\beta = -0.09$), reflecting the progressing impairment of that functional cortical connectivity in the general relation with the worsening of cognitive performance. Furthermore, both DMN and PCC functional connectivity measures also exhibited a significant Group effect pointing to reduced functional cortical connectivity in the “positive” aMCI subgroup (i.e., prodromal AD) compared with the “negative” aMCI subgroup regardless of Time (DMN: $p = 0.01$, Std $\beta = -0.2$; PCC: $p = 0.001$, Std $\beta = -0.3$), reflecting the greater impairment of that functional cortical connectivity in the former than the latter subgroup. Figure 1 (upper diagrams) illustrates these Group and Time effects of functional connectivity in PCC. The plot displays the mean modeled connectivity in the two subgroups of aMCI patients over the 5 recording sessions. The profile of DMN changes is very similar (results not shown). As it can be seen in Fig. 1 for PCC, the functional connectivity decay in the time interval of the study is similar in both subgroups, which is consistent with the finding of no significant Time × Group interactions in DMN and PCC.

Interestingly, only functional cortical connectivity in the LPC node showed a significant Time × Group interaction, indicating an increase of connectivity over time in the “positive” (i.e., prodromal AD) relative to the “negative” aMCI subgroup ($p = 0.01$, Std $\beta = 0.2$). Figure 2 (upper diagram) illustrates the mean values of rsfMRI connectivity in LPC in the “positive” (i.e., prodromal AD) and “negative” aMCI subgroups over the 5 recording sessions.

The attention LFP network showed no Group effect or Group × Time interaction ($p > 0.05$). Indeed, the only significant finding was a Time effect indicating a lower functional cortical connectivity over time in

the LFP network in both “positive” and “negative” aMCI subgroups ($p = 0.01$, Std $\beta = -0.1$).

RsEEG and ERP measures of cortical neural synchronization in the PharmaCog aMCI patients

Table 5 reports the results of a Linear Mixed Model showing the variance explained in rsEEG and ERP measures of cortical neural synchronization (i.e., functional biomarkers) by the fixed effects of Group (“positive” versus “negative” aMCI subgroups as defined by CSF A β ₄₂/P-tau ratio), Time, and Time × Group interaction in the PharmaCog aMCI patients over the observation time (24 months, 5 recording sessions 6 months apart). The main interest was focused on the significant Group and Time × Group interaction effects ($p < 0.05$).

Concerning the significant Group effect, 13 rsEEG biomarkers showed higher cortical source activation in the “positive” (i.e., prodromal AD) over the “negative” aMCI subgroup ($p < 0.05$) for frequency bands and ratios (e.g., delta, theta, delta/alpha1, and theta/alpha1) typically associated with abnormally high values in AD patients. The strongest statistical effects were found on global cortical sources of delta rsEEG rhythms ($p = 0.005$, Std $\beta = 0.3$) and limbic cortical sources of theta rsEEG rhythms ($p = 0.004$, Std $\beta = 0.3$). This effect was independent of Time (i.e., the 5 recording sessions). In the same line, two auditory “oddball” ERP biomarkers also pointed to significant Group effects regardless of Time (e.g., P3b peak as difference between ERPs associated with rare minus frequent stimuli). Compared to the “negative” aMCI subgroup, the “positive” aMCI subgroup (i.e., prodromal AD) pointed to lower cortical source activation of P3b peak in posterior parietal ($p = 0.005$,

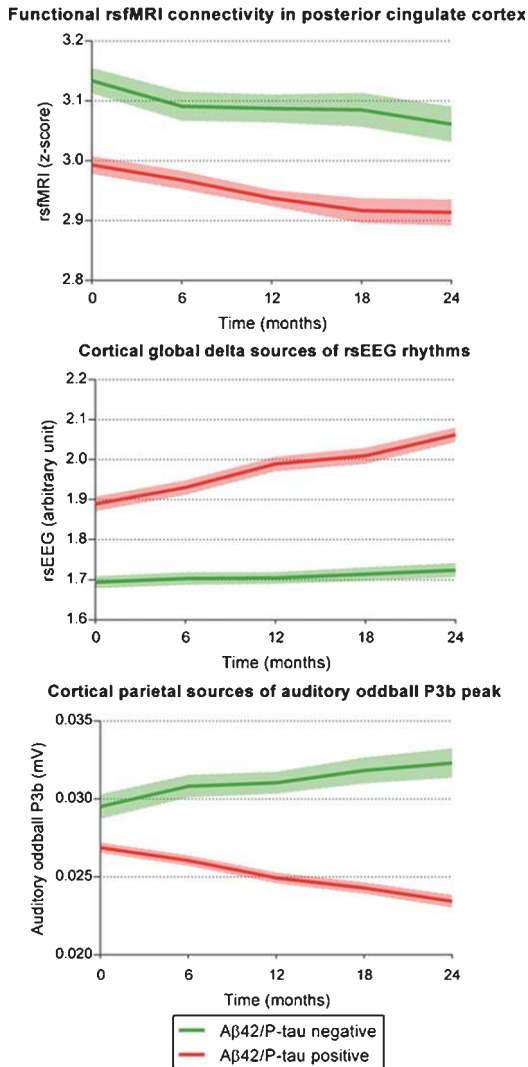


Fig. 1. Longitudinal profile of functional topographical biomarkers showing significant Group effects regardless of time ($p < 0.05$). Patients were stratified in two amnesic mild cognitive impairment (aMCI) subgroups: $A\beta_{42}/P$ -tau “positive” (red) as prodromal AD as an experimental subgroup and $A\beta_{42}/P$ -tau “negative” (green) as a control subgroup. Mean (\pm standard error of the mean, SEM) model values are shown from 5 recording sessions starting at time zero (baseline) and 6-, 12-, 18-, and 24-month follow-ups. Top: resting state functional magnetic resonance imaging (rsfMRI) functional connectivity measures in the precuneus and posterior cingulate cortex (PCC) of the DMN. Of note, functional rsfMRI connectivity in both PCC and global default mode network (DMN; not shown) gave a similar pattern of significant Group effects (connectivity reduction in “positive” group regardless of time) and Time effects (functional decay in Time regardless of Group, $p < 0.05$). Middle: Mean (\pm standard error of the mean, SEM) values of global cortical sources of resting state electroencephalographic (rsEEG) rhythms at delta frequency band (< 4 Hz). Bottom: mean (\pm SEM) values of parietal cortical sources of auditory “oddball” event-related potentials (ERPs) peaking at about 400 ms (P3b peak) post-stimulus following rare minus frequent stimuli in those groups.

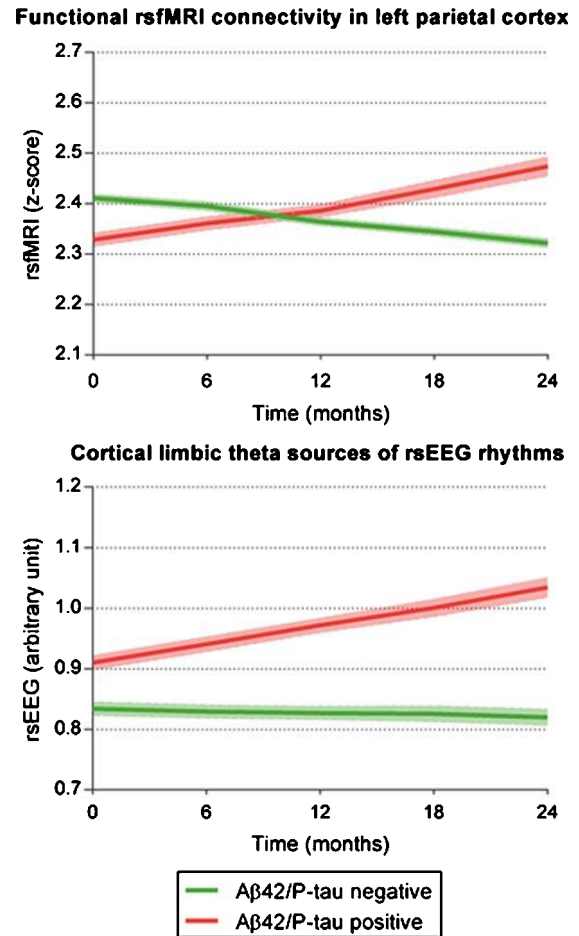


Fig. 2. Longitudinal profile of functional topographical biomarkers showing significant Time \times Group effects ($p < 0.05$). Patients were stratified in two aMCI groups: $A\beta_{42}/P$ -tau “positive” (red) as prodromal AD and $A\beta_{42}/P$ -tau “negative” (green) as a control group. Mean (\pm standard error of the mean, SEM) model values are shown from 5 recording sessions starting at time zero (baseline) and 6-, 12-, 18-, and 24-month follow-ups. Time \times Group effects show differential progression in the two groups. Top: rsfMRI functional connectivity measures in the left parietal cortex (LPC) of the DMN, showing a progression towards increased connectivity in the “positive” aMCI subgroup relative to the “negative” aMCI subgroup. Bottom: Mean (\pm SEM) values of cortical limbic sources of rsEEG rhythms at theta frequency band (4–8 Hz), showing an increase in cortical neural synchronization in the “positive” (i.e., prodromal AD) subgroup relative to the “negative” aMCI control subgroup.

Std $\beta = -0.3$) and posterior cingulate ($p = 0.004$, Std $\beta = -0.2$) regions. Figure 1 (lower diagrams) illustrates the mean values of global cortical sources of delta rsEEG rhythms and cortical source activation of P3b peak in posterior parietal regions in the two subgroups of PharmaCog aMCI patients over the 5 recording sessions.

Table 5

Resting state EEG and auditory oddball ERP measures showing significant cortical neural synchronization effects explained by a Linear Mixed Model of longitudinal changes (baseline, 6, 12, 18, 24 months follow ups) in aMCI patients stratified into two groups (“positive” as prodromal AD and “negative” as a control group)

rsEEG/ERP measures	Group		Time		Time × Group	
	Std β	<i>p</i>	Std β	<i>p</i>	Std β	<i>p</i>
Central delta rsEEG	0.243	0.014	-0.031	0.515	0.124	0.165
Temporal delta rsEEG	0.228	0.044	0.027	0.563	0.054	0.540
Limbic delta rsEEG	0.235	0.031	0.045	0.292	0.056	0.485
Global delta rsEEG	0.296	0.005	0.000	0.991	0.110	0.145
Limbic theta rsEEG	0.263	0.004	-0.017	0.633	0.138	0.046
LGlobal theta rsEEG	0.232	0.020	-0.021	0.602	0.118	0.124
Parietal delta/alpha1 rsEEG	0.212	0.038	-0.056	0.159	0.107	0.156
Frontal theta/alpha1 rsEEG	0.201	0.045	0.003	0.950	0.059	0.513
Central theta/alpha1 rsEEG	0.266	0.009	-0.020	0.639	0.119	0.132
Occipital theta/alpha1 rsEEG	0.188	0.049	-0.067	0.103	0.146	0.060
Temporal theta/alpha1 rsEEG	0.234	0.016	-0.049	0.258	0.138	0.095
Limbic theta/alpha1 rsEEG	0.256	0.010	-0.013	0.756	0.134	0.088
Global theta/alpha1 rsEEG	0.246	0.013	-0.037	0.390	0.134	0.099
Parietal P3b peak	-0.277	0.005	0.030	0.549	-0.162	0.085
Posterior cingulate P3b peak	-0.250	0.017	0.031	0.598	-0.166	0.136

ERP component of interest was the P3b peak as difference between ERPs peaking about 400 ms post-stimulus associated with rare minus frequent stimuli. The model included Group (Aβ42/P-tau ratio), Time, and Time × Group interaction as main predictors of interest adjusted by age, sex and baseline MMSE score as nuisance variables. Significant (*p* < 0.05) fixed effects are emphasized in bold. Std β, standardized β coefficient of the Linear Mixed Model.

587 Concerning the Time × Group interaction (differ-
 588 ential progression between “positive” and “negative”
 589 subgroups of aMCI patients), only limbic sources
 590 of theta rsEEG rhythms showed a significant effect
 591 (*p* = 0.046, Std β = 0.1). Results pointed to a dif-
 592 ferential increase of activation in limbic sources
 593 of theta rhythms over time in the “positive” (i.e.,
 594 prodromal AD) compared to the “negative” aMCI
 595 subgroup (*p* < 0.05). Figure 2 (bottom) depicts the
 596 mean (±SEM) values of those sources in the two
 597 subgroups of aMCI patients over the 5 recording
 598 sessions.

599 *Correlation of rsfMRI and EEG markers with*
 600 *ADAS-cog13 score in the PharmaCog aMCI*
 601 *patients*

602 Linear Mixed Models were also used to test
 603 the correlation of rsfMRI and rsEEG/ERP func-
 604 tional biomarkers with ADAS-cog13 scores in the

605 whole PharmaCog aMCI group (all CSF Aβ42/P-
 606 tau “positive” and “negative” aMCI patients) and
 607 only “positive” aMCI patients (i.e., prodromal AD).
 608 These models were used to test whether those func-
 609 tional biomarkers correlated with a steeper cognitive
 610 decline over time (as assessed by ADAS-cog13
 611 scores) in the “positive” (i.e., prodromal AD) than
 612 “negative” aMCI subgroup. As expected, regardless
 613 the kind of the functional biomarkers, the Time effect
 614 explained an increase of ADAS-cog13 scores (i.e.,
 615 sign of reduced cognitive performance) in the whole
 616 group of the aMCI patients over the observation time
 617 (*p* < 0.001).

618 For rsfMRI biomarkers, the increase of ADAS-
 619 cog13 score was significantly correlated with a reduc-
 620 tion of functional cortical connectivity measured
 621 in DMN (*p* < 0.003, whole aMCI group; *p* < 0.002,
 622 CSF Aβ42/P-tau “positive” aMCI subgroup), PCC
 623 (*p* < 0.004, whole aMCI group; *p* < 0.003, CSF
 624 Aβ42/P-tau “positive” aMCI subgroup), and LFP

network ($p < 0.032$, CSF A β_{42} /P-tau “positive” aMCI subgroup).

For rsEEG-ERP biomarkers, the increase of ADAS-cog13 score was significantly correlated with an increased activation (i.e., neural synchronization) of occipital sources of theta/alpha 1 rsEEG rhythms in the “positive” aMCI subgroup (i.e., prodromal AD; $p = 0.041$), these rhythms being typically augmented in magnitude in AD patients.

As a control analysis, Linear Mixed Models were used for the study of the correlation between rsEEG/ERP functional biomarkers and ADAScog13 score in all PharmaCog aMCI patients without the random intercept and random slope as random effects (namely, without removing the global whole group trend in the worsening of the ADAScog 13 scores over time). The Linear Mixed Models were adjusted for age, sex, and education. Results showed that many rsEEG (e.g., central delta, limbic delta, global delta, limbic theta, global theta, frontal theta/alpha 1, central theta/alpha 1, temporal theta/alpha 1, limbic theta/alpha 1, and occipital theta/alpha 1) and ERP (e.g., parietal and posterior cingulate cortex) functional biomarkers of cortical neural synchronization in the quiet wakefulness (rsEEG) and oddball cognitive task (ERPs) pointed to a significant correlation with ADAS-cog13 score measured over the 5 recording sessions ($p < 0.001$). This control finding remarks the substantial impact of the use of random intercept and random slope as random effects in the present Linear Mixed Models, thus unveiled the strict relationship of the mentioned rsEEG and ERP readouts of cortical neural synchronization with the group worsening of the ADAScog 13 scores over time in the whole PharmaCog population of aMCI patients.

DISCUSSION

Functional topographic biomarkers are of interest because they may reflect early interactions between neuropathological alterations specific to prodromal AD (e.g., extracellular accumulation of A β_{1-42} and intracellular aggregation of P-tau in the brain) and the neurophysiological mechanisms of functional cortical connectivity and neural synchronization as measured by rsfMRI and EEG readouts, respectively. In the present longitudinal PharmaCog study, we evaluated rsfMRI and rsEEG/ERP functional topographic biomarkers to characterize those neurophysiological mechanisms in aMCI patients satisfying the recent diagnostic criteria of prodromal

AD based on CSF biomarkers [1, 66], compared with aMCI patients possibly due to other pathologies. These patients were followed during a relatively long observation period of 24 months.

Functional biomarkers Group effects

The Linear Mixed Models showed a fixed effect of Group (“positive” versus “negative” aMCI subgroups) on both rsfMRI and EEG (i.e., rsEEG and auditory “oddball” ERPs) topographic biomarkers regardless of Time effects. From a general neurophysiological point of view, this finding suggests that the prodromal AD group can be differentiated from the non-prodromal aMCI group by intrinsic functional connectivity and cortical neural synchronization differences (i.e., at rest), as well as by synchronization differences during the oddball task.

Concerning rsfMRI topographic biomarkers, functional connectivity within the DMN, especially within the PCC, was significantly lower in the “positive” (i.e., prodromal AD) than in the “negative” aMCI subgroup regardless of Time effects, while no group difference was observed in the attention LFP network. This finding complements and extends to the prodromal AD condition a large body of previous rsfMRI evidence of cross-sectional studies pointing to a selective disruption of functional connectivity in DMN regions as possible early functional consequences of amyloid-neurodegenerative cascade on cortical systems underpinning resting state condition and low vigilance in AD patients relative to cognitively intact controls ([23, 67–73]; for review, see [74]). As a novelty, the present finding showed a selective disruption of functional connectivity within DMN regions (no difference at an attention frontoparietal network) using a longitudinal study design with several serial recording sessions and a relatively large sample of aMCI patients suffering from prodromal AD ($n = 81$) compared with control aMCI patients not due to AD. Such a control group made the present finding on prodromal AD independent of patients’ cognitive grade (i.e., all patients suffered from an aMCI condition), while the longitudinal design with variable intercepts as random effects minimized the confound of patients’ disease stage in the comparison of the two aMCI subgroups. The present finding has also the robustness of international multicentric studies using harmonized and qualified MRI scanners [49].

On the whole, the design of the present study overcomes the methodological limitations of typical

cross-sectional studies comparing biomarkers in cognitively intact subjects and AD patients. Furthermore, it overcomes the methodological limitations of longitudinal studies just based on one follow up (typically after 1 year). On the other hand, some of the methodological limitations of this study have been previously discussed [49]. In particular, the harmonization of the rsfMRI acquisitions across the 3T Consortium resulted in a common acquisition rate of TR = 2.7 s for full brain coverage. Full brain sub-second acquisition protocols [54] are possible with simultaneous multi-slice selection techniques, which are becoming more widely available as product sequences in clinical scanners and maybe preferable in future studies. The use of higher temporal resolution protocols may improve not only the sensitivity and specificity of rsfMRI connectivity estimates but also enable the exploration of advanced markers of cortical network dynamics [76–78].

The rsfMRI and rsEEG recordings of this study were not recorded simultaneously. However, the results from both modalities refer to a very similar patients' psychophysiological condition as induced by instructions to the patients about the "resting state condition", based on a shared standard operating procedure among the PharmaCog recording units. Indeed, lower/increased level of vigilance, directed attention, and global mental efforts during the resting state condition are clearly related to the brain activity reflected by the present rsfMRI and EEG variables [63, 79].

Concerning rsEEG topographic biomarkers, the present Linear Mixed Models showed a fixed effect of Group ("positive" and "negative" aMCI) on several variables of interest. Compared with the "negative" aMCI subgroup, the "positive" (i.e., prodromal AD) aMCI subgroup exhibited lower posterior (parietal, occipital, temporal and limbic) source activity of the low-frequency alpha band (8–10.5 Hz) while widespread delta (<4 Hz) and theta (4–8 Hz) source activity was higher. These results specify in source space and prodromal AD condition a bulk of previous rsEEG evidence showing that AD patients with dementia are characterized by high power in widespread delta and theta rhythms, as well as low power in posterior alpha and/or beta (13–20 Hz) rhythms [25, 31, 32, 45, 80–82]. In temporal areas, delta power is also abnormally high in AD patients with dementia in relation to regional hypometabolism and memory deficits [83]. Furthermore, a short-term cholinergic regimen with acetylcholinesterase inhibitors partially normalizes theta [84], alpha [85],

and delta [86] rhythms. In the same line, long-term administration of the drug regimen shows beneficial effects on theta and alpha/theta band ratio, especially over the frontal areas [87, 88].

Concerning ERP topographic biomarkers, the Linear Mixed Models showed a fixed effect of Group ("positive" and "negative" aMCI) on P3b peak of an auditory "oddball" paradigm. Compared with the "negative" aMCI subgroup, the "positive" (i.e., prodromal AD) aMCI subgroup pointed to lower parietal and posterior cingulate source activities. These findings extend to spatial source localization previous evidence showing that P3b peak amplitude at scalp posterior electrodes was smaller in AD patients than control seniors, as a possible dynamic neural underpinning of abnormal attention and short-term episodic memory information processes. However, these findings did not replicate in the two aMCI subgroups previous slowing of P3b peak latency in aMCI and AD patients with dementia compared with elderly control subjects, even across various "oddball" task difficulties and stimulus modalities [37, 89–91]. Those effects were previously discussed as related to AD pathology for visual and olfactory modalities [20, 92]. In contrast, the present findings would suggest that P3b peak latency may preferably reflect physiological aging [93] and general deterioration of cognitive performance across pathological aging rather than specific processes of prodromal AD.

Functional biomarkers Time × Group effects: Differential progression profiles

Here the Linear Mixed Models showed a significant interaction between Time (5 recording sessions 6 months apart) and Group ("positive" and "negative" aMCI) on both rsfMRI and rsEEG biomarkers. This interaction suggests that in an aMCI group, differential progression profiles between prodromal and non-prodromal AD may be captured by intrinsic functional connectivity (e.g., rsfMRI biomarkers) and cortical neural synchronization (e.g., rsEEG biomarkers).

Concerning rsfMRI biomarkers, we found that the sensitivity to disease progression in aMCI patients varies across cortical networks. Specifically, we found that functional connectivity in the whole DMN, PCC, and LFP were sensitive to short-term longitudinal decay both in the "positive" prodromal AD and the "negative" (control) aMCI patients. But these networks showed no significant differences in the progression of the connectivity profiles.

826 Instead, functional connectivity in LPC exhibited
827 significant differential effects, with increased func-
828 tional connectivity over time faster in the “positive”
829 (i.e., prodromal AD) relative to the “negative” aMCI
830 subgroup. Again, this finding stressed the selective
831 feature of this disruption of functional connectiv-
832 ity within DMN regions as compared to the lack of
833 effects in the attention frontoparietal network.

834 Our longitudinal rsfMRI findings are in good
835 agreement with previous evidence showing both cor-
836 tical network impairment (connectivity reduction)
837 and compensation (connectivity increase) effects in
838 the DMN in aMCI subjects relative to control seniors,
839 despite gray matter atrophy [54, 94–96]. Here we
840 extend those results by confirming similar effects in
841 prodromal AD relative to control aMCI subgroup.
842 Further, the present findings showed a maximum
843 sensitivity of rsfMRI LPC functional connectivity at
844 2-year follow up, generally consistent with previous
845 longitudinal rsfMRI studies considering baseline and
846 2–3 year follow-up evaluations in groups of patients
847 with AD dementia and aMCI [54–56, 96], the latter
848 sometimes diagnosed only on clinical basis. Inter-
849 estingly, the present lateralization in the left LPC
850 of the effects of longitudinal disease progression in
851 prodromal AD extends recent findings of a longitu-
852 dinal rsfMRI study with two measurements 2 years
853 apart in a small population of aMCI patients [95].
854 Such previous study exhibited sensitivity of func-
855 tional connectivity between left precuneus and other
856 DMN nodes in accounting for the greater progres-
857 sion of aMCI patients in the group of converters to
858 dementia ($n = 14$) than that of non-converters ($n = 17$)
859 [95]. Another recent longitudinal rsfMRI study (base-
860 line and 35 month follow up) in aMCI patients
861 evaluated genotype-by-diagnosis interaction effects
862 [23, 97]. Using seed-based rsfMRI analyses on the
863 hippocampus, the Authors detected functional cor-
864 tical connectivity reductions in APOE $\epsilon 4$ carriers
865 and functional cortical connectivity increases in non-
866 carriers. In the light of those findings, the present
867 results should not be interpreted as an indication that
868 rsfMRI functional biomarkers of prodromal AD are
869 limited to DMN nodes. It is reasonable that functional
870 connectivity within the episodic memory brain net-
871 works including prefrontal, entorhinal regions, and
872 hippocampus may represent another sensitive dimen-
873 sion in prodromal AD.

874 Concerning rsEEG biomarkers, the “positive” (i.e.,
875 prodromal AD) aMCI subgroup was characterized
876 by increasing limbic source activity of theta rhythms
877 over time. The effect was evident across the serial

878 recordings and robust effects were evident for the
879 progression of prodromal AD in periods of about 12
880 months. Taking into account the relatively low spatial
881 resolution of the EEG techniques used in the present
882 study (i.e., they cannot disentangle the various limbic
883 regions of cortical midline and medial temporal
884 lobe), this finding suggests a limbic localization of
885 prodromal AD processes affecting the generation of
886 abnormal rsEEG rhythms during the disease progres-
887 sion in aMCI patients. This topographical suggestion
888 is in line with the well-known localization of initial
889 AD physiopathological processes in entorhinal
890 regions, medial temporal lobe, and midline regions
891 of DMN. Furthermore, it provides a neuroanatomical
892 framework to previous rsEEG evidence showing
893 that AD patients with dementia are characterized by
894 high power in widespread scalp regions of delta and
895 theta rhythms, as well as low power in posterior alpha
896 and/or beta (13–20 Hz) rhythms [27, 28, 32, 98, 99].

897 *What do rsfMRI and EEG topographic* 898 *biomarkers tell us about prodromal AD?*

899 The rsfMRI findings of the present study support
900 the general view that at least for two years, pro-
901 dromal AD is associated with a partial functional
902 cortical disconnection within DMN nodes in the rest-
903 ing state condition. It can be speculated that this
904 functional disconnection might induce an abnormal
905 elaboration of information about self-body milieu and
906 autobiographical memory, thus affecting the sense
907 of self-awareness and continuity of self across time
908 [6, 77] (for theories and controversies about the neural
909 basis of consciousness see [101]). This speculation is
910 based on the well-known concept that midline cortical
911 nodes of DMN such as PCC and MPF contribute
912 to the integration of the general functions related to
913 the sense of self-awareness [102, 103]. In this line
914 of reasoning, PCC might represent information con-
915 cerning individual’s own self-beliefs and first-person
916 perspective in adults [104]. Furthermore, structural
917 maturation of the neural connectivity between PCC
918 and MPF in the adolescence accompanies the devel-
919 opment of self-related and social-cognitive functions
920 [105]. Moreover, previous evidence has shown that
921 posterior parietal regions of DMN might contribute
922 to the formation of self-related cognitive represen-
923 tation as a convergence zone binding cortical neural
924 populations involved in the memorization of inter-
925 modal details of episodic events concerning the
926 self [106]. Patients with lesions in those parietal
927 regions manifest difficulties in re-experiencing a past

928 autobiographic event when request by experimenters
929 [107]. This speculation encourages the inclusion of
930 cognitive tests probing the richness of the autobio-
931 graphic memories and self-awareness in prodromal
932 AD patients over time and the analysis with Linear
933 Mixed Models of the correlation between rsfMRI
934 topographic biomarkers of DMN and the perfor-
935 mance to those tests.

936 The rsEEG findings of the present study enlight-
937 ened neurophysiological mechanisms characterizing
938 prodromal AD patients compared to control aMCI
939 patients. Based on those findings and prior knowledge
940 on the role of thalamocortical loops in the generation
941 of rsEEG rhythms in humans, it can be speculated
942 that in quiet wakefulness, the abnormal delta and
943 theta source activity in prodromal AD is due to an
944 abnormal interaction between thalamic and cortical
945 pyramidal neural populations, associated with a loss
946 of functional connectivity and a sort of functional
947 isolation of parietal, temporal, and occipital cortical
948 modules [108–110]. It can be also speculated that
949 the alteration of this neurophysiological mechanism
950 is responsible for the reduced parietal and poste-
951 rior cingulate source activity of auditory “oddball”
952 P3b peak in prodromal AD patients enrolled in the
953 present study. Indeed, P3b peak is mostly an expres-
954 sion of cognitive event-related oscillatory response
955 of thalamocortical circuits oscillating at delta and
956 theta frequencies. In this line, previous studies have
957 shown that delta event-related impulse oscillations
958 in response to visual and auditory “oddball” stim-
959 uli were attenuated in amplitude in AD patients with
960 dementia compared with control seniors (see for a
961 review [111]). In AD patients with dementia, an
962 abnormal thalamocortical interaction might be due
963 to a cortical blood hypoperfusion and synaptic dys-
964 function [83, 112–119]. Another cause of such an
965 abnormal thalamocortical interaction might be an
966 impairment of the cortical gray matter especially in
967 the posterior regions [29, 39, 120–126], as well as a
968 lesion in the brain white matter connecting cerebral
969 cortex [2, 23].

970 Another interesting finding of the present study
971 is the characterization of prodromal AD patients by
972 widespread cortical alpha sources estimated in the
973 resting state condition in the wakefulness. A tentative
974 neurophysiological explanation of that finding can be
975 based on the insightful research in cats and mice per-
976 formed by the group of Dr. Crunelli at the Cardiff
977 University. Based on their research, it can be spec-
978 ulated that the reduction of cortical alpha sources in
979 prodromal AD patients over aMCI control patients

980 might denote a progressive alteration in the inter-
981 play of thalamocortical high-threshold, GABAergic
982 (interneurons), thalamocortical relay-mode, and cor-
983 tical pyramidal neurons that constitute the complex
984 network regulating the cortical arousal and vigilance
985 in quiet wakefulness in mammals [107–109].
986 In physiological conditions, Dr. Crunelli’s group
987 demonstrated that in wakefulness, glutamatergic and
988 cholinergic signaling to those neurons enhances the
989 generation of thalamocortical and cortical alpha
990 rhythms and produces cycles of excitation and inhibi-
991 tion in thalamic and cortical neurons that might frame
992 perceptual events in discrete snapshots of approxi-
993 mately 70–100 ms during vigilance [107–109].

994 What is the added value of the present rsfMRI and
995 EEG readouts with reference to the new diagnostic
996 guidelines for research published by the Interna-
997 tional Working Group-2 [1] and NIA-AA Working
998 Group [66]? Summarizing, those guidelines stated
999 that AD can be recognized *in vivo* by both abnor-
1000 mal “A” biomarkers of A β and “T” biomarkers of
1001 phospho tau in the brain, derived from PET or CSF
1002 techniques. Furthermore, the new NIA-AA Working
1003 Group [66] proposed that early “AD neuropatho-
1004 logic changes” can be revealed *in vivo* by abnormal
1005 “A” biomarkers of A β and normal “T” biomarkers.
1006 Finally, both International Working Group-2 [1] and
1007 NIA-AA Working Group [66] encouraged the char-
1008 acterization of AD subject’s brain integrity by “N”
1009 biomarkers of neurodegeneration derived from CSF
1010 (e.g., T-tau), FDG-PET (e.g., hypometabolism), and
1011 structural MRI (e.g., atrophy) techniques. In the Phar-
1012 maCog project, we followed those guidelines for the
1013 diagnosis of the prodromal AD in aMCI patients. As
1014 a novelty, here we propose that the present rsfMRI
1015 and rsEEG readouts changing over time (e.g., 24
1016 months) in prodromal AD patients may be used to
1017 characterize and monitor the effect of the disease
1018 on their brain functions, thus enriching the picture
1019 disclosed by the guideline biomarkers. Specifically,
1020 these readouts may complement “N” biomarkers in
1021 future longitudinal clinical studies, revealing effects
1022 of the prodromal AD progression and new anti-AD
1023 drugs on brain functional connectivity with high spa-
1024 tial resolution (i.e., probing fine spatial features of
1025 the functional brain topography) and neural synchro-
1026 nization processes with high temporal resolution (i.e.,
1027 probing multiple oscillatory features of that syn-
1028 chronization facilitating or inhibiting neural signal
1029 processing), respectively. Relative neurophysiologi-
1030 cal insights may better explain clinical manifestations
1031 of the disease and therapy response beyond diagnostic

and prognostic purposes. Of note, the present article appears in an editorial Mini Forum of the *Journal of Alzheimer's Disease* together with other articles derived from the same PharmaCog clinical trial. One of these articles reports results of systematic statistical comparisons among structural and functional MRI, rsEEG/ERP, and blood biomarkers in prodromal AD patients.

CONCLUSIONS

In the PharmaCog project, auditory “oddball” ERPs, rsEEG, and rsfMRI functional biomarkers were tested in aMCI patients to characterize prodromal AD. The prodromal AD in patients with aMCI was established based on abnormal CSF levels of amyloid and P-tau measured at baseline. To take into account the confounding effect of different disease stages and cognitive grades, we used 5 serial recording sessions over 2 years, controlling of cognitive grade using a control group of aMCI patients supposed not due to AD. Functional biomarkers were able to detect significant Group effects stable over time in the prodromal AD patients compared with the control aMCI subgroup: 1) reduced rsfMRI functional connectivity in the DMN and in the PCC node; 2) increased rsEEG source activity at delta (<4 Hz) and theta (4–8 Hz) rhythms and decreased source activity at alpha (8–10.5 Hz) rhythms; and 3) reduced parietal and posterior cingulate source activities of P3b peak of ERPs. Functional biomarkers were also able to show Time × Group effects, giving differential progression profiles over time in the prodromal AD subgroup relative to the control aMCI subgroup: 1) increased rsfMRI functional connectivity in the LPC node of the DMN and 2) increased limbic source activity at theta rhythms. Topographical biomarkers may have different sensitivity at different phases of the disease [1, 127]. At the present stage, we do not know the neuropathological correlates explaining why some rsfMRI and EEG biomarkers were found to be sensitive to Group effects and others to Group × Time effects over 24 months. Future studies correlating those biomarkers with PET maps of Aβ_{1–42} and P-tau accumulation in the brain may enlighten such an explanation. The effects observed in this study may be related to the progression of the neurodegeneration shown by 1) FDG-PET maps of hypometabolism in parietal and medial temporal cortical areas, 2) atrophy of hippocampus, entorhinal, and temporal neocortex, and 3) biomarkers of tau

aggregation in the brain as revealed by CSF samples and PET maps.

The present findings represent the first longitudinal characterization of functional topographic biomarkers of prodromal AD. If cross-validated, these findings may be used for the stratification and monitoring of the effects of disease-modifying drugs in aMCI patients suffering from AD. Indeed, topographic biomarkers of brain function as those derived from rsfMRI and EEG (or the magnetoencephalographic counterpart) may be more likely to respond to an effective disease-modifying intervention relative to structural neuroimaging atrophy markers (e.g., cortical or hippocampus atrophy) or topographic biomarkers of brain hypometabolism (e.g., those measured by FDG-PET), which may only partially recover as they are markedly dependent on neurodegeneration [1].

ACKNOWLEDGMENTS

This study has been carried out in the Work Package 5 of PharmaCog project (2010–2015, Grant no. 115009; <http://www.pharmacog.org>). The PharmaCog project was funded by the Innovative Medicine Initiative of European Seventh Framework Program, which was granted by the European Committee (50%) and the European Federation of Pharmaceutical Industries and Associations (50%).

Dr. Giovanni Frisoni's group was supported for the development of this study and extraction of magnetic resonance image (MRI) biomarkers by an in-kind contribution of AstraZeneca AB, Södertälje, Sweden.

Dr. Claudio Babiloni's group was also supported for the extraction of electroencephalographic (EEG) biomarkers by an in-kind contribution of F. Hoffmann-La Roche, Basel, Switzerland.

The Authors are grateful to all members and collaborators of the PharmaCog project and to all amnesic mild cognitive impairment (aMCI) patients who agreed to participate in this study as well as the healthy elderly volunteers who participated in the preliminary harmonization phase of the study.

Authors' disclosures available online (<https://www.j-alz.com/manuscript-disclosures/18-0158r1>).

REFERENCES

- [1] Dubois B, Feldman HH, Jacova C, Hampel H, Molinuevo JL, Blennow K, DeKosky ST, Gauthier S, Selkoe D, Bateman R, Cappa S, Crutch S, Engelborghs S, Frisoni GB, Fox NC, Galasko D, Habert MO, Jicha GA, Nordberg A,

- 1129 Pasquier F, Rabinovici G, Robert P, Rowe C, Salloway S,
 1130 Sarazin M, Epelbaum S, de Souza LC, Vellas B, Visser PJ,
 1131 Schneider L, Stern Y, Scheltens P, Cummings JL (2014)
 1132 Advancing research diagnostic criteria for Alzheimer's
 1133 disease: The IWG-2 criteria. *Lancet Neurol* **13**,
 1134 614-629.
- 1135 [2] Agosta F, Scola E, Canu E, Marcone A, Magnani G, Sarro
 1136 L, Copetti M, Caso F, Cerami C, Comi G, Cappa SF,
 1137 Falini A, Filippi M (2012) White matter damage in fronto-
 1138 temporal lobar degeneration spectrum. *Cereb Cortex* **22**,
 1139 2705-2714.
- 1140 [3] Friston KJ (2009) Modalities, modes, and models in func-
 1141 tional neuroimaging. *Science* **326**, 399-403.
- 1142 [4] Sporns O (2013) Structure and function of complex brain
 1143 networks. *Dialogues Clin Neurosci* **15**, 247-262.
- 1144 [5] Deco G, Tononi G, Boly M, Kringelbach ML (2015)
 1145 Rethinking segregation and integration: Contributions of
 1146 whole-brain modelling. *Nat Rev Neurosci* **16**, 430-439.
- 1147 [6] Biswal B, Yetkin FZ, Haughton VM, Hyde JS (1995)
 1148 Functional connectivity in the motor cortex of resting
 1149 human brain using echo-planar MRI. *Magn Reson Med*
 1150 **34**, 537-541.
- 1151 [7] Fox MD, Raichle ME (2007) Spontaneous fluctuations
 1152 in brain activity observed with functional magnetic res-
 1153 onance imaging. *Nat Rev Neurosci* **8**, 700-711.
- 1154 [8] Heine L, Soddu A, Gómez F, Vanhaudenhuyse A,
 1155 Tshibanda L, Thonnard M, Charland-Verville V, Kirsch
 1156 M, Laureys S, Demertzi A (2012) Resting state networks
 1157 and consciousness: Alterations of multiple resting state
 1158 network connectivity in physiological, pharmacological,
 1159 and pathological consciousness States. *Front Psychol* **3**,
 1160 295.
- 1161 [9] Johnson SC, Baxter LC, Wilder LS, Pipe JG, Heis-
 1162 erman JE, Prigatano GP (2002) Neural correlates of
 1163 self-reflection. *Brain* **125**, 1808-1814.
- 1164 [10] Lou HC, Luber B, Crupain M, Keenan JP, Nowak M, Kjaer
 1165 TW, Sackeim HA, Lisanby SH (2004) Parietal cortex and
 1166 representation of the mental Self. *Proc Natl Acad Sci U S
 1167 A* **101**, 6827-6832.
- 1168 [11] Gusnard DA, Akbudak E, Shulman GL, Raichle ME
 1169 (2001) Medial prefrontal cortex and self-referential men-
 1170 tal activity: Relation to a default mode of brain function.
 1171 *Proc Natl Acad Sci U S A* **98**, 4259-4264.
- 1172 [12] Sheline YI, Barch DM, Price JL, Rundle MM, Vaish-
 1173 navi SN, Snyder AZ, Mintun MA, Wang S, Coalson RS,
 1174 Raichle ME (2009) The default mode network and self-
 1175 referential processes in depression. *Proc Natl Acad Sci
 1176 U S A* **106**, 1942-1947.
- 1177 [13] McKiernan KA, D'Angelo BR, Kaufman JN, Binder JR
 1178 (2006) Interrupting the "stream of consciousness": An
 1179 fMRI investigation. *Neuroimage* **29**, 1185-1191.
- 1180 [14] Mason MF, Norton MI, Van Horn JD, Wegner DM,
 1181 Grafton ST, Macrae CN (2007) Wandering minds: The
 1182 default network and stimulus-independent thought. *Sci-
 1183 ence* **315**, 393-395.
- 1184 [15] Goldberg II, Harel M, Malach R (2006) When the brain
 1185 loses its self: Prefrontal inactivation during sensorimotor
 1186 processing. *Neuron* **50**, 329-339.
- 1187 [16] Greicius MD, Krasnow B, Reiss AL, Menon V (2003)
 1188 Functional connectivity in the resting brain: A network
 1189 analysis of the default mode hypothesis. *Proc Natl Acad
 1190 Sci U S A* **100**, 253-258.
- 1191 [17] Raichle ME, MacLeod AM, Snyder AZ, Powers WJ, Gus-
 1192 nard DA, Shulman GL (2001) A default mode of brain
 1193 function. *Proc Natl Acad Sci U S A* **98**, 676-682.
- [18] Raichle ME, Snyder AZ (2007) A default mode of brain
 1194 function: A brief history of an evolving idea. *Neuroimage*
 1195 **37**, 1083-1090.
- [19] Buckner RL, Andrews-Hanna JR, Schacter DL (2008) The
 1196 brain's default network: Anatomy, function, and relevance
 1197 to disease. *Ann N Y Acad Sci* **1124**, 1-38.
- [20] Polich J, Pitzer A (1999) P300 and Alzheimer's disease:
 1200 Oddball task difficulty and modality effects. *Electroen-
 1201 cephalogr Clin Neurophysiol Suppl* **50**, 281-287.
- [21] Clifford JO, Anand S (1997) Tri-axial recording of event-
 1202 related potentials during passive cognitive tasks in patients
 1203 with Alzheimer's disease. *Int J Neurosci* **92**, 29-45.
- [22] Babiloni C, Lizio R, Marzano N, Capotosto P, Soricelli
 1204 A, Triggiani AI, Cordone S, Gesualdo L, Del Percio C
 1205 (2016) Brain neural synchronization and functional cou-
 1206 pling in Alzheimer's disease as revealed by resting state
 1207 EEG rhythms. *Int J Psychophysiol* **103**, 88-102.
- [23] Agosta F, Dalla Libera D, Spinelli EG, Finardi A, Canu
 1208 E, Bergami A, Bocchio Chiavetto L, Baronio M, Comi G,
 1209 Martino G, Matteoli M, Magnani G, Verderio C, Furlan
 1210 R (2014) Myeloid microvesicles in cerebrospinal fluid are
 1211 associated with myelin damage and neuronal loss in mild
 1212 cognitive impairment and Alzheimer disease. *Ann Neurol*
 1213 **76**, 813-825.
- [24] Koenig T, Pritchep L, Dierks T, Hubl D, Wahlund LO,
 1214 John ER, Jelic V (2005) Decreased EEG synchronization
 1215 in Alzheimer's disease and mild cognitive impairment.
 1216 *Neurobiol Aging* **26**, 165-171.
- [25] Babiloni C, Binetti G, Cassetta E, Dal Forno G, Del Per-
 1217 cio C, Ferreri F, Ferri R, Frisoni G, Hirata K, Lanuzza B,
 1218 Miniussi C, Moretti D V, Nobili F, Rodriguez G, Romani
 1219 GL, Salinari S, Rossini PM (2006) Sources of cortical
 1220 rhythms change as a function of cognitive impairment in
 1221 pathological aging: A multicenter study. *Clin Neurophys-
 1222 iol* **117**, 252-268.
- [26] Babiloni C, Cassetta E, Binetti G, Tombini M, Del Percio
 1223 C, Ferreri F, Ferri R, Frisoni G, Lanuzza B, Nobili F, Parisi
 1224 L, Rodriguez G, Frigerio L, Gurzi M, Prestia A, Vernieri
 1225 F, Eusebi F, Rossini PM (2007) Resting EEG sources cor-
 1226 relate with attentional span in mild cognitive impairment
 1227 and Alzheimer's disease. *Eur J Neurosci* **25**, 3742-3757.
- [27] Babiloni C, Del Percio C, Lizio R, Marzano N, Infarinato
 1228 F, Soricelli A, Salvatore E, Ferri R, Bonforte C, Tedeschi
 1229 G, Montella P, Baglieri A, Rodriguez G, Fama F, Nobili
 1230 F, Vernieri F, Ursini F, Mundi C, Frisoni GB, Rossini PM
 1231 (2014) Cortical sources of resting state electroencephalo-
 1232 graphic alpha rhythms deteriorate across time in subjects
 1233 with amnesic mild cognitive impairment. *Neurobiol Aging*
 1234 **35**, 130-142.
- [28] Babiloni C, Lizio R, Del Percio C, Marzano N, Soricelli A,
 1235 Salvatore E, Ferri R, Cosentino FI, Tedeschi G, Montella
 1236 P, Marino S, De Salvo S, Rodriguez G, Nobili F, Vernieri
 1237 F, Ursini F, Mundi C, Richardson JC, Frisoni GB, Rossini
 1238 PM (2013) Cortical sources of resting state EEG rhythms
 1239 are sensitive to the progression of early stage Alzheimer's
 1240 disease. *J Alzheimers Dis* **34**, 1015-1035.
- [29] Babiloni C, Vecchio F, Del Percio C, Montagnese S, Schif-
 1241 f S, Lizio R, Chini G, Serviddio G, Marzano N, Soricelli A,
 1242 Frisoni GB, Rossini PM, Amodio P (2013) Resting state
 1243 cortical electroencephalographic rhythms in covert hepatic
 1244 encephalopathy and Alzheimer's disease. *J Alzheimers Dis*
 1245 **34**, 707-725.
- [30] Babiloni C, Vecchio F, Lizio R, Ferri R, Rodriguez G,
 1246 Marzano N, Frisoni GB, Rossini PM (2011) Resting
 1247 state cortical rhythms in mild cognitive impairment and
 1248 1249 1250 1251 1252 1253 1254 1255 1256 1257 1258

- Alzheimer's disease: Electroencephalographic evidence. *J Alzheimers Dis* **26**(Suppl 3), 201-214.
- [31] Huang C, Wahlund L, Dierks T, Julin P, Winblad B, Jelic V (2000) Discrimination of Alzheimer's disease and mild cognitive impairment by equivalent EEG sources: A cross-sectional and longitudinal study. *Clin Neurophysiol* **111**, 1961-1967.
- [32] Jelic V, Johansson SE, Almkvist O, Shigeta M, Julin P, Nordberg A, Winblad B, Wahlund LO (2000) Quantitative electroencephalography in mild cognitive impairment: Longitudinal changes and possible prediction of Alzheimer's disease. *Neurobiol Aging* **21**, 533-540.
- [33] Jervis BW, Belal S, Cassar T, Besleaga M, Bigan C, Michalopoulos K, Zervakis M, Camilleri K, Fabri S (2010) Waveform analysis of non-oscillatory independent components in single-trial auditory event-related activity in healthy subjects and Alzheimer's disease patients. *Curr Alzheimer Res* **7**, 334-347.
- [34] Papaliagkas V, Kimiskidis V, Tsolaki M, Anogianakis G (2008) Usefulness of event-related potentials in the assessment of mild cognitive impairment. *BMC Neurosci* **9**, 107.
- [35] Papaliagkas VT, Anogianakis G, Tsolaki MN, Koliakos G, Kimiskidis VK (2010) Combination of P300 and CSF beta-amyloid(1-42) assays may provide a potential tool in the early diagnosis of Alzheimer's disease. *Curr Alzheimer Res* **7**, 295-299.
- [36] Papaliagkas VT, Kimiskidis VK, Tsolaki MN, Anogianakis G (2011) Cognitive event-related potentials: Longitudinal changes in mild cognitive impairment. *Clin Neurophysiol* **122**, 1322-1326.
- [37] Polich J, Corey-Bloom J (2005) Alzheimer's disease and P300: Review and evaluation of task and modality. *Curr Alzheimer Res* **2**, 515-525.
- [38] Tsolaki AC, Kosmidou V, Kompatsiaris IY, Papadaniil C, Hadjileontiadis L, Adam A, Tsolaki M (2017) Brain source localization of MMN and P300 ERPs in mild cognitive impairment and Alzheimer's disease: A high-density EEG approach. *Neurobiol Aging* **55**, 190-201.
- [39] Babiloni C, Del Percio C, Boccardi M, Lizio R, Lopez S, Carducci F, Marzano N, Soricelli A, Ferri R, Triggiani AI, Prestia A, Salinari S, Rasser PE, Basar E, Fama F, Nobili F, Yener G, Emek-Savas DD, Gesualdo L, Mundi C, Thompson PM, Rossini PM, Frisoni GB (2015) Occipital sources of resting-state alpha rhythms are related to local gray matter density in subjects with amnesic mild cognitive impairment and Alzheimer's disease. *Neurobiol Aging* **36**, 556-570.
- [40] Babiloni C, Del Percio C, Caroli A, Salvatore E, Nicolai E, Marzano N, Lizio R, Cavedo E, Landau S, Chen K, Jagust W, Reiman E, Tedeschi G, Montella P, De Stefano M, Gesualdo L, Frisoni GB, Soricelli A (2016) Cortical sources of resting state EEG rhythms are related to brain hypometabolism in subjects with Alzheimer's disease: An EEG-PET study. *Neurobiol Aging* **48**, 122-134.
- [41] Babiloni C, Frisoni G, Steriade M, Bresciani L, Binetti G, Del Percio C, Geroldi C, Miniussi C, Nobili F, Rodriguez G, Zappasodi F, Carfagna T, Rossini PM (2006) Frontal white matter volume and delta EEG sources negatively correlate in awake subjects with mild cognitive impairment and Alzheimer's disease. *Clin Neurophysiol* **117**, 1113-1129.
- [42] Babiloni C, Pievani M, Vecchio F, Geroldi C, Eusebi F, Fracassi C, Fletcher E, De Carli C, Boccardi M, Rossini PM, Frisoni GB (2009) White-matter lesions along the cholinergic tracts are related to cortical sources of EEG rhythms in amnesic mild cognitive impairment. *Hum Brain Mapp* **30**, 1431-1443.
- [43] Czigler B, Csikos D, Hidasi Z, Anna Gaal Z, Csibri E, Kiss E, Salacz P, Molnar M (2008) Quantitative EEG in early Alzheimer's disease patients - power spectrum and complexity features. *Int J Psychophysiol* **68**, 75-80.
- [44] Jelles B, Scheltens P, van der Flier WM, Jonkman EJ, da Silva FH, Stam CJ (2008) Global dynamical analysis of the EEG in Alzheimer's disease: Frequency-specific changes of functional interactions. *Clin Neurophysiol* **119**, 837-841.
- [45] Jeong J (2004) EEG dynamics in patients with Alzheimer's disease. *Clin Neurophysiol* **115**, 1490-1505.
- [46] Albi A, Pasternak O, Minati L, Marizzoni M, Bartres-Faz D, Bargallo N, Bosch B, Rossini PM, Marra C, Muller B, Fiedler U, Wiltfang J, Roccatagliata L, Picco A, Nobili FM, Blin O, Sein J, Ranjeva JP, Didic M, Bombois S, Lopes R, Bordet R, Gros-Dagnac H, Payoux P, Zoccatelli G, Alessandrini F, Beltramello A, Ferretti A, Caulo M, Aiello M, Cavaliere C, Soricelli A, Parnetti L, Tarducci R, Floridi P, Tsolaki M, Constantinidis M, Drevelegas A, Frisoni G, Jovicich J (2017) Free water elimination improves test-retest reproducibility of diffusion tensor imaging indices in the brain: A longitudinal multisite study of healthy elderly subjects. *Hum Brain Mapp* **38**, 12-26.
- [47] Jovicich J, Marizzoni M, Bosch B, Bartres-Faz D, Arnold J, Benninghoff J, Wiltfang J, Roccatagliata L, Picco A, Nobili F, Blin O, Bombois S, Lopes R, Bordet R, Chanoine V, Ranjeva JP, Didic M, Gros-Dagnac H, Payoux P, Zoccatelli G, Alessandrini F, Beltramello A, Bargallo N, Ferretti A, Caulo M, Aiello M, Ragucci M, Soricelli A, Salvadori N, Tarducci R, Floridi P, Tsolaki M, Constantinidis M, Drevelegas A, Rossini PM, Marra C, Otto J, Reiss-Zimmermann M, Hoffmann KT, Galluzzi S, Frisoni GB (2014) Multisite longitudinal reliability of tract-based spatial statistics in diffusion tensor imaging of healthy elderly subjects. *Neuroimage* **101**, 390-403.
- [48] Jovicich J, Marizzoni M, Sala-Llonch R, Bosch B, Bartres-Faz D, Arnold J, Benninghoff J, Wiltfang J, Roccatagliata L, Nobili F, Hensch T, Trankner A, Schonknecht P, Leroy M, Lopes R, Bordet R, Chanoine V, Ranjeva JP, Didic M, Gros-Dagnac H, Payoux P, Zoccatelli G, Alessandrini F, Beltramello A, Bargallo N, Blin O, Frisoni GB (2013) Brain morphometry reproducibility in multi-center 3T MRI studies: A comparison of cross-sectional and longitudinal segmentations. *Neuroimage* **83**, 472-484.
- [49] Jovicich J, Minati L, Marizzoni M, Marchitelli R, Sala-Llonch R, Bartres-Faz D, Arnold J, Benninghoff J, Fiedler U, Roccatagliata L, Picco A, Nobili F, Blin O, Bombois S, Lopes R, Bordet R, Sein J, Ranjeva JP, Didic M, Gros-Dagnac H, Payoux P, Zoccatelli G, Alessandrini F, Beltramello A, Bargallo N, Ferretti A, Caulo M, Aiello M, Cavaliere C, Soricelli A, Parnetti L, Tarducci R, Floridi P, Tsolaki M, Constantinidis M, Drevelegas A, Rossini PM, Marra C, Schonknecht P, Hensch T, Hoffmann KT, Kuijjer JP, Visser PJ, Barkhof F, Frisoni GB (2016) Longitudinal reproducibility of default-mode network connectivity in healthy elderly participants: A multicentric resting-state fMRI study. *Neuroimage* **124**, 442-454.
- [50] Marchitelli R, Minati L, Marizzoni M, Bosch B, Bartres-Faz D, Muller BW, Wiltfang J, Fiedler U, Roccatagliata L, Picco A, Nobili F, Blin O, Bombois S, Lopes R, Bordet R, Sein J, Ranjeva JP, Didic M, Gros-Dagnac H, Payoux P, Zoccatelli G, Alessandrini F, Beltramello A, Bargallo N, Ferretti A, Caulo M, Aiello M, Cavaliere C, Soricelli A,

- 1389 Parnetti L, Tarducci R, Floridi P, Tsolaki M, Constantinidis
1390 M, Drevelegas A, Rossini PM, Marra C, Schonknecht P,
1391 Hensch T, Hoffmann KT, Kuijper JP, Visser PJ, Barkhof
1392 F, Frisoni GB, Jovicich J (2016) Test-retest reliability
1393 of the default mode network in a multi-centric fMRI
1394 study of healthy elderly: Effects of data-driven physio-
1395 logical noise correction techniques. *Hum Brain Mapp* **37**,
1396 2114-2132.
- [51] Marizzoni M, Antelmi L, Bosch B, Bartres-Faz D, Muller
1397 BW, Wiltfang J, Fiedler U, Roccatagliata L, Picco A,
1398 Nobili F, Blin O, Bombois S, Lopes R, Sein J, Ranjeva
1399 JP, Didic M, Gros-Dagnac H, Payoux P, Zoccatelli
1400 G, Alessandrini F, Beltramello A, Bargallo N, Ferretti
1401 A, Caulo M, Aiello M, Cavaliere C, Soricelli A, Sal-
1402 vadori N, Parnetti L, Tarducci R, Floridi P, Tsolaki M,
1403 Constantinidis M, Drevelegas A, Rossini PM, Marra C,
1404 Hoffmann KT, Hensch T, Schonknecht P, Kuijper JP, Visser
1405 PJ, Barkhof F, Bordet R, Frisoni GB, Jovicich J (2015)
1406 Longitudinal reproducibility of automatically segmented
1407 hippocampal subfields: A multisite European 3T study on
1408 healthy elderly. *Hum Brain Mapp* **36**, 3516-3527.
- [52] Galluzzi S, Marizzoni M, Babiloni C, Albani D, Antelmi
1410 L, Bagnoli C, Bartres-Faz D, Cordone S, Didic M, Farotti
1411 L, Fiedler U, Forloni G, Girtler N, Hensch T, Jovicich
1412 J, Leeuwis A, Marra C, Molinuevo JL, Nobili F, Parie-
1413 nte J, Parnetti L, Payoux P, Del Percio C, Ranjeva JP,
1414 Rolandi E, Rossini PM, Schonknecht P, Soricelli A, Tso-
1415 laki M, Visser PJ, Wiltfang J, Richardson JC, Bordet R,
1416 Blin O, Frisoni GB (2016) Clinical and biomarker profil-
1417 ing of prodromal Alzheimer's disease in workpackage 5
1418 of the Innovative Medicines Initiative PharmaCog project:
1419 A "European ADNI study." *J Intern Med* **279**, 576-591.
- [53] Nathan PJ, Lim YY, Abbott R, Galluzzi S, Marizzoni M,
1421 Babiloni C, Albani D, Bartres-Faz D, Didic M, Farotti L,
1422 Parnetti L, Salvadori N, Muller BW, Forloni G, Girtler N,
1423 Hensch T, Jovicich J, Leeuwis A, Marra C, Molinuevo
1424 JL, Nobili F, Pariente J, Payoux P, Ranjeva JP, Rolandi
1425 E, Rossini PM, Schonknecht P, Soricelli A, Tsolaki M,
1426 Visser PJ, Wiltfang J, Richardson JC, Bordet R, Blin O,
1427 Frisoni GB (2017) Association between CSF biomarkers,
1428 hippocampal volume and cognitive function in patients
1429 with amnesic mild cognitive impairment (MCI). *Neuro-
1430 biol Aging* **53**, 1-10.
- [54] Damoiseaux JS (2012) Resting-state fMRI as a biomarker
1432 for Alzheimer's disease? *Alzheimers Res Ther* **4**, 8.
- [55] Damoiseaux JS, Prater KE, Miller BL, Greicius MD
1433 (2012) Functional connectivity tracks clinical deteriora-
1434 tion in Alzheimer's disease. *Neurobiol Aging* **33**, 828
1435 e19-30.
- [56] Binnewijzend MA, Schoonheim MM, Sanz-Arigitia E,
1437 Wink AM, van der Flier WM, Tolboom N, Adriaanse SM,
1438 Damoiseaux JS, Scheltens P, van Berckel BN, Barkhof
1439 F (2012) Resting-state fMRI changes in Alzheimer's dis-
1440 ease and mild cognitive impairment. *Neurobiol Aging* **33**,
1441 2018-2028.
- [57] Dennis EL, Thompson PM (2014) Functional brain con-
1443 nectivity using fMRI in aging and Alzheimer's disease.
1444 *Neuropsychol Rev* **24**, 49-62.
- [58] Franzmeier N, Gottler J, Grimmer T, Drzezga A, Araque-
1446 Caballero MA, Simon-Vermot L, Taylor ANW, Burger
1447 K, Catak C, Janowitz D, Muller C, Duering M, Sorg
1448 C, Ewers M (2017) Resting-state connectivity of the left
1449 frontal cortex to the default mode and dorsal attention net-
1450 work supports reserve in mild cognitive impairment. *Front
1451 Aging Neurosci* **9**, 264.
- [59] Calhoun VD, Adali T, Pearson GD, Pekar JJ (2001) A
1452 method for making group inferences from functional MRI
1453 data using independent component analysis. *Hum Brain
1454 Mapp* **14**, 140-151.
- [60] Moretti D V, Babiloni F, Carducci F, Cincotti F, Remondini
1456 E, Rossini PM, Salinari S, Babiloni C (2003) Com-
1457 puterized processing of EEG-EOG-EMG artifacts for
1458 multi-centric studies in EEG oscillations and event-related
1459 potentials. *Int J Psychophysiol* **47**, 199-216.
- [61] Pascual-Marqui (2007) Discrete, 3D distributed, linear
1461 imaging methods of electric neuronal activity. Part 1:
1462 Exact, zero error localization. *Clin Neurophysiol* **112**, 7.
- [62] Clifford JO, Williston JS (1992) Three dimensional vector
1464 analysis of the spatial components and voltage magnitudes
1465 of the P300 response during different attentional states and
1466 stimulus modalities. *Int J Psychophysiol* **12**, 1-10.
- [63] Clifford JO, Williston JS (1993) The effects of attention
1468 and context on the spatial and magnitude components of
1469 the early responses of the event-related potential elicited
1470 by a rare stimulus. *Int J Psychophysiol* **14**, 209-226.
- [64] Kickhefel A, Weiss C, Roland J, Gross P, Schick F, Salomir
1472 R (2012) Correction of susceptibility-induced GRE phase
1473 shift for accurate PRFS thermometry proximal to cryoab-
1474 lation iceball. *Magn Reson Mater Physics Biol Med* **25**,
1475 23-31.
- [65] Marizzoni M, Ferrari C, Galluzzi S, Jovicich J, Albani D,
1477 Babiloni C, Didic M, Forloni G, Molinuevo JL, Nobili
1478 FM, Parnetti L, Payoux P, Rossini PM, Schönknecht P,
1479 Soricelli A, Tsolaki M, Visser PJ, Wiltfang J, Bordet R,
1480 Cavaliere L, Richardson J, Blin O, Frisoni GB (2017) CSF
1481 biomarkers and effect of apolipoprotein E genotype, age
1482 and sex on cut-off derivation in mild cognitive impairment.
1483 *Alzheimers Dement*. **13**, P1319.
- [66] Jack CR, Bennett DA, Blennow K, Carrillo MC, Dunn
1485 B, Haeberlein SB, Holtzman DM, Jagust W, Jessen F,
1486 Karlawish J, Liu E, Molinuevo JL, Montine T, Phelps C,
1487 Rankin KP, Rowe CB, Scheltens P, Siemers E, Snyder
1488 HM, Sperling R, Contributors C, Masliah E, Ryan L, Sil-
1489 verberg N (2018) NIA-AA Research Framework: Toward
1490 a biological definition of Alzheimer's disease. *Alzheimers
1491 Dement* **14**, 535-562.
- [67] Zhang HY, Wang SJ, Liu B, Ma ZL, Yang M, Zhang ZJ,
1493 Teng GJ (2010) Resting brain connectivity: Changes dur-
1494 ing the progress of Alzheimer disease. *Radiology* **256**,
1495 598-606.
- [68] Gili T, Cercignani M, Serra L, Perri R, Giove F, Mar-
1497 aviglia B, Caltagirone C, Bozzali M (2011) Regional brain
1498 atrophy and functional disconnection across Alzheimer's
1499 disease evolution. *J Neurol Neurosurg Psychiatry* **82**, 58-
1500 66.
- [69] Lau WK, Leung MK, Lee TM, Law AC (2016) Resting-
1502 state abnormalities in amnesic mild cognitive impairment:
1503 A meta-analysis. *Transl Psychiatry* **6**, e790.
- [70] Petrella JR, Sheldon FC, Prince SE, Calhoun VD,
1505 Doraiswamy PM (2011) Default mode network connec-
1506 tivity in stable vs progressive mild cognitive impairment.
1507 *Neurology* **76**, 511-517.
- [71] Song J, Qin W, Liu Y, Duan Y, Liu J, He X, Li K, Zhang
1509 X, Jiang T, Yu C (2013) Aberrant functional organization
1510 within and between resting-state networks in AD. *PLoS
1511 One* **8**, e63727.
- [72] Mieva H, Letenneur L, Dartigues J-F, Rouch-Leroyer I,
1513 Sourgen C, D'Alchee-Biree F, Dib M, Barberger-Gateau
1514 P, Orgogozo J-M, Fabrigoule C (2004) Annual rate and
1515 predictors of conversion to dementia in subjects presenting
1516

- mild cognitive impairment criteria defined according to a population-based study. *Dement Geriatr Cogn Disord* **18**, 87-93.
- [73] Geifman N, Brinton RD, Kennedy RE, Schneider LS, Butte AJ (2017) Evidence for benefit of statins to modify cognitive decline and risk in Alzheimer's disease. *Alzheimers Res Ther* **9**, 10.
- [74] Zhou J, Liu S, Ng KK, Wang J (2017) Applications of resting-state functional connectivity to neurodegenerative disease. *Neuroimaging Clin N Am* **27**, 663-683.
- [75] Feinberg DA, Moeller S, Smith SM, Auerbach E, Ramanna S, Gunther M, Glasser MF, Miller KL, Ugurbil K, Yacoub E (2010) Multiplexed echo planar imaging for sub-second whole brain fMRI and fast diffusion imaging. *PLoS One* **5**, e15710.
- [76] de Pasquale F, Corbetta M, Betti V, Della Penna S (2018) Cortical cores in network dynamics. *Neuroimage* **180**(Pt B), 370-382.
- [77] Preibisch C, Castrillon GJ, Buhner M, Riedl V (2015) Evaluation of multiband EPI acquisitions for resting state fMRI. *PLoS One* **10**, e0136961.
- [78] Wig GS (2017) Segregated systems of human brain networks. *Trends Cogn Sci* **21**, 981-996.
- [79] Schwartz S, Vuilleumier P, Hutton C, Maravita A, Dolan RJ, Driver J (2005) Attentional load and sensory competition in human vision: Modulation of fMRI responses by load at fixation during task-irrelevant stimulation in the peripheral visual field. *Cereb Cortex* **15**, 770-786.
- [80] Dierks T, Ihl R, Frolich L, Maurer K (1993) Dementia of the Alzheimer type: Effects on the spontaneous EEG described by dipole sources. *Psychiatry Res* **50**, 151-162.
- [81] Dierks T, Jelic V, Pascual-Marqui RD, Wahlund L, Julin P, Linden DE, Maurer K, Winblad B, Nordberg A (2000) Spatial pattern of cerebral glucose metabolism (PET) correlates with localization of intracerebral EEG-generators in Alzheimer's disease. *Clin Neurophysiol* **111**, 1817-1824.
- [82] Ponomareva NV, Selesneva ND, Jarikov GA (2003) EEG alterations in subjects at high familial risk for Alzheimer's disease. *Neuropsychobiology* **48**, 152-159.
- [83] Valladares-Neto DC, Buchsbaum MS, Evans WJ, Nguyen D, Nguyen P, Siegel B V, Stanley J, Starr A, Guich S, Rice D (1995) EEG delta, positron emission tomography, and memory deficit in Alzheimer's disease. *Neuropsychobiology* **31**, 173-181.
- [84] Brassen S, Adler G (2003) Short-term effects of acetylcholinesterase inhibitor treatment on EEG and memory performance in Alzheimer patients: An open, controlled trial. *Pharmacopsychiatry* **36**, 304-308.
- [85] Onofrij M, Thomas A, Iacono D, Luciano AL, Di Iorio A (2003) The effects of a cholinesterase inhibitor are prominent in patients with fluctuating cognition: A part 3 study of the main mechanism of cholinesterase inhibitors in dementia. *Clin Neuropharmacol* **26**, 239-251.
- [86] Reeves RR, Struve FA, Patrick G (2002) The effects of donepezil on quantitative EEG in patients with Alzheimer's disease. *Clin Electroencephalogr* **33**, 93-96.
- [87] Kogan EA, Korczyn AD, Virchovsky RG, Klimovizky Ss, Treves TA, Neufeld MY (2001) EEG changes during long-term treatment with donepezil in Alzheimer's disease patients. *J Neural Transm* **108**, 1167-1173.
- [88] Rodriguez G, Vitali P, De Leo C, De Carli F, Girtler N, Nobili F (2002) Quantitative EEG changes in Alzheimer patients during long-term donepezil therapy. *Neuropsychobiology* **46**, 49-56.
- [89] Golob EJ, Irimajiri R, Starr A (2007) Auditory cortical activity in amnesic mild cognitive impairment: Relationship to subtype and conversion to dementia. *Brain* **130**, 740-752.
- [90] Polich J, Comerchero MD (2003) P3a from visual stimuli: Typicality, task, and topography. *Brain Topogr* **15**, 141-152.
- [91] Rossini PM, Rossi S, Babiloni C, Polich J (2007) Clinical neurophysiology of aging brain: From normal aging to neurodegeneration. *Prog Neurobiol* **83**, 375-400.
- [92] Morgan CD, Murphy C (2002) Olfactory event-related potentials in Alzheimer's disease. *J Int Neuropsychol Soc* **8**, 753-763.
- [93] van Dinteren R, Arns M, Jongsma MLA, Kessels RPC (2014) P300 development across the lifespan: A systematic review and meta-analysis. *PLoS One* **9**, e87347.
- [94] Qi Z, Wu X, Wang Z, Zhang N, Dong H, Yao L, Li K (2010) Impairment and compensation coexist in amnesic MCI default mode network. *Neuroimage* **50**, 48-55.
- [95] Serra L, Cercignani M, Mastropasqua C, Torso M, Spano B, Makovac E, Viola V, Giulietti G, Marra C, Caltagirone C, Bozzali M (2016) Longitudinal changes in functional brain connectivity predicts conversion to Alzheimer's disease. *J Alzheimers Dis* **51**, 377-389.
- [96] Bai F, Liao W, Watson DR, Shi Y, Yuan Y, Cohen AD, Xie C, Wang Y, Yue C, Teng Y, Wu D, Jia J, Zhang Z (2011) Mapping the altered patterns of cerebellar resting-state function in longitudinal amnesic mild cognitive impairment patients. *J Alzheimers Dis* **23**, 87-99.
- [97] Ye Q, Su F, Shu H, Gong L, Xie CM, Zhou H, Zhang ZJ, Bai F (2017) Shared effects of the clusterin gene on the default mode network among individuals at risk for Alzheimer's disease. *CNS Neurosci Ther* **23**, 395-404.
- [98] Coben LA, Danziger W, Storandt M (1985) A longitudinal EEG study of mild senile dementia of Alzheimer type: Changes at 1 year and at 2.5 years. *Electroencephalogr Clin Neurophysiol* **61**, 101-112.
- [99] Soininen H, Partanen J, Laulumaa V, Helkala EL, Laakso M, Riekkinen PJ (1989) Longitudinal EEG spectral analysis in early stage of Alzheimer's disease. *Electroencephalogr Clin Neurophysiol* **72**, 290-297.
- [100] Weiler M, Northoff G, Damasceno BP, Balthazar MLF (2016) Self, cortical midline structures and the resting state: Implications for Alzheimer's disease. *Neurosci Biobehav Rev* **68**, 245-255.
- [101] Tegmark M (2000) Importance of quantum decoherence in brain processes. *Phys Rev E Stat Phys Plasmas Fluids Relat Interdiscip Topics* **61**, 4194-206.
- [102] Northoff G, Bermpohl F (2004) Cortical midline structures and the self. *Trends Cogn Sci* **8**, 102-107.
- [103] Northoff G, Heinzel A, de Greck M, Bermpohl F, Dobrowolny H, Panksepp J (2006) Self-referential processing in our brain—a meta-analysis of imaging studies on the self. *Neuroimage* **31**, 440-457.
- [104] Ochsner KN, Beer JS, Robertson ER, Cooper JC, Gabrieli JD, Kihlstrom JF, D'Esposito M (2005) The neural correlates of direct and reflected self-knowledge. *Neuroimage* **28**, 797-814.
- [105] Supekar K, Uddin LQ, Prater K, Amin H, Greicius MD, Menon V (2010) Development of functional and structural connectivity within the default mode network in young children. *Neuroimage* **52**, 290-301.
- [106] Shimamura AP (2011) Episodic retrieval and the cortical binding of relational activity. *Cogn Affect Behav Neurosci* **11**, 277-291.

- 1649 [107] Berryhill ME (2012) Insights from neuropsychology: Pin- 1691
1650 pointing the role of the posterior parietal cortex in episodic 1692
1651 and working memory. *Front Integr Neurosci* **6**, 31. 1693
- 1652 [108] Klimesch W (1999) EEG alpha and theta oscillations 1694
1653 reflect cognitive and memory performance: A review and 1695
1654 analysis. *Brain Res Brain Res Rev* **29**, 169-195. 1696
- 1655 [109] Pfurtscheller G, Lopes da Silva FH (1999) Event-related 1697
1656 EEG/MEG synchronization and desynchronization: Basic 1698
1657 principles. *Clin Neurophysiol* **110**, 1842-1857. 1699
- 1658 [110] Steriade M, Llinas RR (1988) The functional states of the 1700
1659 thalamus and the associated neuronal interplay. *Physiol*
1660 *Rev* **68**, 649-742. 1701
- 1661 [111] Yener GG, Basar E (2013) Biomarkers in Alzheimer's dis- 1702
1662 ease with a special emphasis on event-related oscillatory 1703
1663 responses. *Suppl Clin Neurophysiol* **62**, 237-273. 1704
- 1664 [112] Rae-Grant A, Blume W, Lau C, Hachinski VC, Fis- 1705
1665 man M, Merskey H (1987) The electroencephalogram in 1706
1666 Alzheimer-type dementia. A sequential study correlating 1707
1667 the electroencephalogram with psychometric and quanti- 1708
1668 tative pathologic data. *Arch Neurol* **44**, 50-54. 1709
- 1669 [113] Brenner RP, Ulrich RF, Spiker DG, Scwabassi RJ, Reynolds 1710
1670 3rd CF, Marin RS, Boller F (1986) Computerized 1711
1671 EEG spectral analysis in elderly normal, demented and 1712
1672 depressed subjects. *Electroencephalogr Clin Neurophysiol* **64**, 483-492. 1713
- 1673 [114] Stigsby B, Johannesson G, Ingvar DH (1981) Regional 1714
1674 EEG analysis and regional cerebral blood flow in 1715
1675 Alzheimer's and Pick's diseases. *Electroencephalogr Clin*
1676 *Neurophysiol* **51**, 537-547. 1716
- 1677 [115] Kwa VI, Weinstein HC, Posthumus Meyjes EF, van Royen 1717
1678 EA, Bour LJ, Verhoeff PN, Ongerboer de Visser BW 1718
1679 (1993) Spectral analysis of the EEG and 99m-Tc-HMPAO 1719
1680 SPECT-scan in Alzheimer's disease. *Biol Psychiatry* **33**, 1720
1681 100-107. 1721
- 1682 [116] Niedermeyer E (1997) Alpha rhythms as physiological and 1722
1683 abnormal phenomena. *Int J Psychophysiol* **26**, 31-49. 1723
- 1684 [117] Passero S, Rocchi R, Vatti G, Burgalassi L, Battistini N 1724
1685 (1995) Quantitative EEG mapping, regional cerebral blood 1725
1686 flow, and neuropsychological function in Alzheimer's dis- 1726
1687 ease. *Dementia* **6**, 148-156. 1727
- 1688 [118] Rodriguez G, Copello F, Vitali P, Perego G, Nobili F (1999) 1728
1689 EEG spectral profile to stage Alzheimer's disease. *Clin*
1690 *Neurophysiol* **110**, 1831-1837. 1729
- [119] Steriade M (1994) Sleep oscillations and their blockage 1730
by activating systems. *J Psychiatry Neurosci* **19**, 354-358. 1731
- [120] Killiany RJ, Moss MB, Albert MS, Sandor T, Tieman J, 1732
Jolesz F (1993) Temporal lobe regions on magnetic reso-
nance imaging identify patients with early Alzheimer's
disease. *Arch Neurol* **50**, 949-954. 1733
- [121] Fernandez A, Arrazola J, Maestu F, Amo C, Gil-Gregorio 1734
P, Wienbruch C, Ortiz T (2003) Correlations of hip-
pocampal atrophy and focal low-frequency magnetic
activity in Alzheimer disease: Volumetric MR imaging-
magnetoencephalographic study. *AJNR Am J Neuroradiol*
24, 481-487. 1735
- [122] Delli Pizzi S, Maruotti V, Taylor JP, Franciotti R, Caulo 1736
M, Tartaro A, Thomas A, Onofrij M, Bonanni L (2014)
Relevance of subcortical visual pathways disruption to
visual symptoms in dementia with Lewy bodies. *Cortex*
59, 12-21. 1737
- [123] Delli Pizzi S, Franciotti R, Taylor JP, Esposito R, Tartaro 1738
A, Thomas A, Onofrij M, Bonanni L (2015) Structural
connectivity is differently altered in dementia with Lewy body
and Alzheimer's disease. *Front Aging Neurosci* **7**, 208. 1739
- [124] Delli Pizzi S, Padulo C, Brancucci A, Bubbico G, Edden 1740
RA, Ferretti A, Franciotti R, Manippa V, Marzoli D, Onofrij
M, Sepede G, Tartaro A, Tommasi L, Puglisi-Allegra S,
Bonanni L (2016) GABA content within the ventromedial
prefrontal cortex is related to trait anxiety. *Soc Cogn Affect*
Neurosci **11**, 758-766. 1741
- [125] Graff-Radford J, Madhavan M, Vemuri P, Rabinstein AA, 1742
Cha RH, Mielke MM, Kantarci K, Lowe V, Senjem
ML, Gunter JL, Knopman DS, Petersen RC, Jack CR Jr,
Roberts RO (2016) Atrial fibrillation, cognitive impair-
ment, and neuroimaging. *Alzheimers Dement* **12**, 391-398. 1743
- [126] Sarro L, Senjem ML, Lundt ES, Przybelski SA, Lesnick 1744
TG, Graff-Radford J, Boeve BF, Lowe VJ, Ferman TJ,
Knopman DS, Comi G, Filippi M, Petersen RC, Jack
CR Jr, Kantarci K (2016) Amyloid-beta deposition and
regional grey matter atrophy rates in dementia with Lewy
bodies. *Brain* **139**, 2740-2750. 1745
- [127] Frisoni GB, Fox NC, Jack CR, Scheltens P, Thompson PM 1746
(2010) The clinical use of structural MRI in Alzheimer
disease. *Nat Rev Neurol* **6**, 67-77. 1747